

ANALYSIS OF LEAD-FREE AMMUNITION BY SCANNING ELECTRON MICROSCOPY USING ENERGY
DISPERSIVE X-RAY SPECTROSCOPY AND DISCRIMINATION OF SAMPLES USING PRINCIPAL
COMPONENTS ANALYSIS

By

Seth R. Hogg

A THESIS

Submitted to
Michigan State University
in partial fulfillment of the requirements
for the degree of

Forensic Science – MASTER OF SCIENCE

2013

ABSTRACT

ANALYSIS OF LEAD-FREE AMMUNITION BY SCANNING ELECTRON MICROSCOPY USING ENERGY DISPERSIVE X-RAY SPECTROSCOPY AND DISCRIMINATION OF SAMPLES USING MULTIVARIATE STATISTICAL METHODS

By

Seth R. Hogg

Six commonly available brands of non-toxic, 9 mm ammunition as well as the most common brand of road safety flare utilized in the United States were purchased. Five rounds from each box were fired as purchased while five were disassembled allowing firing of only primer components in the presence of three conductive carbon tabs positioned near the weapon muzzle, permitting capture of gunshot residue (GSR). Road flares were burned in the presence of two conductive tabs positioned above the flare to capture any ejected particles during the combustion process.

A carbon tab was analyzed from each of the resulting 61 samples using a scanning electron microscope (SEM). Particles visually consistent with the morphology of GSR were located on the tabs designating the area as a region of interest and all particles within view were analyzed by EDS. Searching of each sample finished after 30 regions of interest were identified. Maximum peak height normalization was applied to the resulting spectra prior to statistical analysis. The pretreated data were then analyzed using principal components analysis (PCA) to investigate association of ammunition by manufacturer, based on the element profiles generated. Then, the association of samples from whole bullets to those from primers only, and the differentiation of actual GSR from a ubiquitous road flare were also investigated using PCA.

Copyright by
SETH R. HOGG
2013

ACKNOWLEDGEMENTS

I want to express my sincerest gratitude to the many people who assisted me in completing this degree. I appreciate the time and advice on data pretreatment and statistical comparisons provided to me by my advisor, Dr. Ruth Smith. Dr. Brian Hunter was also instrumental in this project assisting with firearms knowledge while serving on my committee along with Dr. Thomas Holt. The project also could not succeed without the involvement of Lt. Ron Crichton of the Michigan State Police providing indoor firing range access and overseeing all experiments. I also wish to thank Dr. Baokang Bi for assistance with use of the SEM-EDS system. Additionally, without the encouragement and support of Darlene Grace, ASAC Edward Van Patten, GS Randal Divine, GS Mark Styron, and the rest of the HIDTA team the choice to venture to Michigan would not have come easily. Many thanks to Chuck Wood as well for teaching me what I know of law enforcement.

Likewise, I wish to recognize John McIlroy for his assistance related to data treatment procedures as well as the rest of the members of the Forensic Chemistry program, both past and present, for their suggestions and encouragement.

Finally, I thank my family for their never-ending support and encouragement. From driving me around the country for explorer competitions, to helping me pack up and move cross-country to continue my education, they are always there for me. I am also so thankful to have met Shana Santos. Her passion, strength, and light-heartedness were quintessential to persisting through the many late nights and long hours required to finish this project.

TABLE OF CONTENTS

LIST OF TABLES	vii
LIST OF FIGURES	viii
LIST OF ABBREVIATIONS	x
CHAPTER 1: INTRODUCTION	1
1.1 Justification	1
1.2 Ammunition	3
1.3 Forensic Gunshot Residue Detection	7
1.4 Environmental Sources of Gunshot Residue Like Particles	11
1.5 Research Objectives	13
REFERENCES	15
CHAPTER 2: THEORY	19
2.1 Gunshot Residue Formation	19
2.2 Scanning Electron Microscopy/Energy Dispersive X-ray Spectroscopy	22
2.3 Principal Components Analysis	25
REFERENCES	29
CHAPTER 3: MATERIALS AND METHODS	31
3.1 Experimental Design and Sample Collection	31
3.1.1 Primer Study	31
3.1.2 Intact Ammunition Study	34
3.1.3 Road Safety Flare Study	36
3.2 SEM-EDS Analysis of GSR Particles	37
3.3 Data Processing	38
3.4 Principal Components Analysis of EDS Spectra	40
REFERENCES	43
CHAPTER 4: RESULTS AND DISCUSSION	45
4.1 Introduction	45
4.2 Particle Deposition Observations	46
4.3 Energy Dispersive X-ray Spectroscopy Analysis and Comparison of Spectra	48
4.3.1 Remington UMC Leadless	48
4.3.2 Winchester WinClean	49
4.3.3 Winchester SuperClean NT	51
4.3.4 Magtech Cleanrange	53

4.3.5 CCI Blazer	54
4.3.6 Sellier & Bellot Non-toxic	56
4.3.7 Orion Road Flare	57
4.3.8 Comparison of Ammunition and Road Flare Based on EDS Spectra	58
4.4 Principal Components Analysis	61
4.4.1 Primer Samples and Road Flare	61
4.4.2 Intact Ammunition Samples and Road Flare	65
4.4.3 Complete Dataset and Road Flare	67
REFERENCES	71
 CHAPTER 5: CONCLUSIONS AND FUTURE WORK	 73
5.1 Conclusions	73
5.2 Future Work	75
REFERENCES	77

LIST OF TABLES

Table 4.1: GSR particle counts for each of five replicates for six different intact ammunition and primer samples. Error on the average is reported as \pm one standard deviation. 47

LIST OF FIGURES

Figure 1.1: Components of ammunition	3
Figure 1.2: Boxer and Berdan primer differences	5
Figure 2.1: Schematic of a SEM-EDS system	23
Figure 3.1: Glock 17 slide and barrel after removing barrel length (above) compared to unmodified components from another Glock 17 (below).	32
Figure 3.2: Dual conductive carbon tab placement 15 cm downrange perpendicular to particle trajectory during primer composition studies.	33
Figure 3.3: Ruger KP95DC 9mm pistol supported on firing stand for intact ammunition studies. For interpretation of the references to color in this and all other figures, the reader is referred to the electronic version of this thesis.	35
Figure 3.4: Barrel view downrange through adhesive tabs documenting the bullet trajectory during intact ammunition composition studies.	35
Figure 3.5: Dual conductive carbon tab placement 15 cm downrange (1 parallel, 1 perpendicular) along with a third tab placed 10 cm downrange parallel to bullet trajectory during intact ammunition composition studies.	36
Figure 3.6: Suspected GSR particle located during manual SEM-EDS search at 500x magnification with a 20 keV accelerating voltage in secondary electron imaging mode.	38
Figure 3.7: Representative EDS spectrum for a suspected GSR particle showing elemental contributions from carbon, oxygen, potassium, and calcium.	39
Figure 3.8: Representative EDS spectrum after removing background elemental contributions and empty energy channels.	39
Figure 3.9: EDS spectra for the five replicate (F1-F5) firings of WinSC primers before (A) and after (B) maximum peak normalization.	41
Figure 4.1: EDS spectra for the five replicate (F1-F5) firings of Rem primers (A) and intact ammunition (B) showing an elemental composition of Al, Si, and K, with Al as the dominant peak.	49
Figure 4.2: EDS spectra for the five replicate (F1-F5) firings of WinCl primers (A) and intact ammunition (B) showing an elemental composition of K and Si, K with traces of Na, Mg, Al, S, and Ca.	51
Figure 4.3: EDS spectra for the five replicate (F1-F5) firings of WinSC primers (A) and intact ammunition (B) showing an elemental composition of K and Si with traces of Mg, Al, S, and Ca.	52

- Figure 4.4:** EDS spectra for the five replicate (F1-F5) firings of Mag primers (A) and intact ammunition (B) showing an elemental composition of Al and Si with traces of K and Ca. 54
- Figure 4.5:** EDS spectra for the five replicate (F1-F5) firings of CCI primers (A) and intact ammunition (B) showing an elemental composition of Sr and Al. 55
- Figure 4.6:** EDS spectra for the five replicate (F1-F5) firings of S&B primers (A) and intact ammunition (B) showing an elemental composition of Si with traces of Al, K, and Ca. 57
- Figure 4.7:** EDS spectrum for the particles resulting from burning an ORI flare showing an elemental composition of Sr and S with traces of Cl and K. 58
- Figure 4.8:** Overlaid average EDS spectra comparison of a single replicate trial from each ammunition compared to the ORI spectrum to assess whether road flares may be visually discriminated from lead-free ammunition on the basis of EDS elemental composition. 60
- Figure 4.9:** PCA scores plot showing clustering of replicate primer samples for the six ammunitions and the positioning of the road flare sample. 62
- Figure 4.10:** PCA loadings plots showing each element's contribution to the variance corresponding to PC1 (A) and PC2 (B). 62
- Figure 4.11:** Normalized average EDS spectra for P-Rem showing fifth firing with increased K content. 64
- Figure 4.12:** PCA scores plot showing clustering of intact replicate samples for the six ammunitions and the positioning of the road flare sample. 66
- Figure 4.13:** PCA loadings plots showing contributions to the variance corresponding to PC1 (A) and PC2 (B). 66
- Figure 4.14:** PCA scores plot showing clustering of intact and primer replicate samples for the six ammunitions along with the positioning of the road flare sample. Square symbols denote primer samples while triangles denote intact ammunition samples. 68
- Figure 4.15:** PCA loadings plots showing each element's contribution to the positioning on PC1 (A) and PC2 (B). 68

LIST OF ABBREVIATIONS

GSR	Gunshot Residue
SEM-EDS	Scanning Electron Microscopy – Energy Dispersive X-ray Spectroscopy
PCA	Principal Components Analysis
ICP-MS	Inductively Coupled Plasma Mass Spectrometry
PC	Principal Component
Rem	Remington UMC Leadless 9 mm Luger Ammunition
WinSC	Winchester SuperClean 9 mm Luger Ammunition
WinCI	Winchester WinClean 9 mm Luger Ammunition
Mag	Magtech CleanRange 9 mm Luger Ammunition
CCI	CCI Blazer Clean-Fire 9mm Luger Ammunition
S&B	Sellier & Bellot Nontox 9mm Luger Ammunition
ORI	Orion Safety Products Road Flare
RSD	Relative Standard Deviation
Al	Aluminum
K	Potassium
Si	Silicon
MSDS	Material Safety Data Sheet
Na	Sodium
Ca	Calcium
Mg	Magnesium
S	Sulfur
Sr	Strontium
Cl	Chlorine

CHAPTER 1: INTRODUCTION

1.1 Justification

Upon discharging a firearm, small particles containing elements of the cartridge case, primer mixture, and bullet, are aerosolized. In traditional ammunition, lead is a major component of both the bullet and the primer mixture. Lead readily enters the blood stream through airborne exposure and may lead to negative health effects.^{1,2} Concerns over the toxic byproducts produced by traditional ammunition formulations resulted in the development of new, non-toxic compositions. Among the first of these was the Sintox brand, which was commercially available in 1980, and was designed specifically to restrict the use of heavy metals.³ New primer formulations removed the use of the traditional lead styphnate replacing it with a wide variety of less unique elements such as strontium, potassium, silicon, and titanium. Non-toxic ammunitions also contain bullets either formulated without lead or with a lead core completely coated in a non-toxic metal such as copper.⁴ The new formulations are also manufacturer specific causing much larger compositional variability than is typically observed in traditional ammunitions.

Currently, formal forensic gunshot residue (GSR) analysis requires the presence of lead, barium, and antimony within a single spherical particle with a diameter ranging between hundreds of nanometers to micrometers in order to classify the particle as uniquely originating from the discharge of a firearm.⁵ Through removal of the heavy metals within the primer and bullet compositions, non-toxic ammunition poses a challenge for forensic classification. While

many years of study failed to demonstrate any environmental sources of particles consistent with the lead, barium, and antimony composition and morphology classified as unique to GSR, non-toxic ammunition remains understudied within the forensic community.⁶ Differentiation of particles from non-toxic ammunition and environmental sources such as fireworks and road flares must be adequately addressed in order to confidently assign an origin to a discovered particle in a forensic examination.

Within the 2009 report by the National Research Council of the National Academies of Sciences that detailed suggested improvements to forensic science practices, the need for statistical confidence in forensic results was highlighted.⁷ Only a single paper to date discusses statistical treatment of GSR particle information obtained from scanning electron microscopy with energy dispersive X-ray spectroscopy (SEM-EDS) analysis. The elements considered in the study included silicon, potassium, calcium, antimony, barium, strontium, zinc, titanium, copper, and tin. Fast Fourier transformations were used to reduce the large number of X-ray energy counts monitored by the instrument according to their importance in each spectrum. Regularized discriminant analysis was then used to classify individual GSR particles to 7 brands of non-toxic ammunition with greater than 90% correct classification in all cases.⁸ However, by reducing the number of data points through the fast Fourier transformation, the largest peaks contributed most to particle differentiation and smaller peaks were excluded. Furthermore, there was no attempt to distinguish GSR particles from environmental sources, such as cartridge fired welding tools, road flares, or fireworks.

1.2 Ammunition

Modern handgun ammunition configurations consist of four components assembled into a single self-contained unit. The four components are the case, primer cup, propellant, and bullet (Figure 1.1). Upon pulling the trigger mechanism within a weapon, the hammer is released to strike the firing pin. The firing pin passes through the breech face striking the primer cup causing rapid burning of the primer material. The burning primer components then ignite the propellant leading to the rapid production of gases trapped within the casing. Once a sufficiently high pressure accumulates, the bullet is ejected from the case through the firearm barrel.⁹ As the bullet exits the barrel, gases and small particulate matter, which are termed GSR, are also released from the firearm. GSR consists of a complex mixture of particles originating from the case, primer mixture and cup, propellant, bullet, lubricants, sealants, and the firearm barrel.

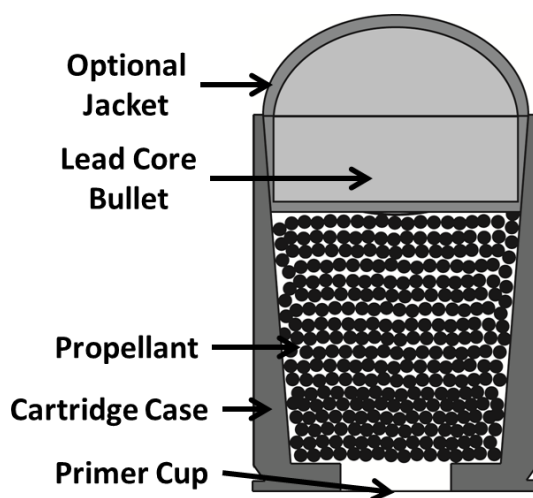


Figure 1.1: Components of ammunition

Cartridge cases must securely restrain the primer, propellant, and bullet in a proper orientation for discharge to allow for safe storage and transport as well as to resist the entrance of moisture or oil. Most cases are composed of brass (30% zinc and 70% copper) but other compositions may include steel, copper, nickel-plated brass, cupronickel (20% nickel and 80% copper), gilding metal (10% zinc and 90% copper), aluminum, or plastic. Upon ignition of the propellant, the rapid release of gases within the case causes its expansion to the firearm chamber walls leading to a tight seal, which directs the majority of the force to propel the bullet down the barrel.⁹

Within common centerfire ammunition, the primer cup sits at the base of the case within the primer pocket held exposed for firing pin access. To detonate the ammunition, the firing pin strikes the primer cup and initiates combustion of the sensitive self-contained primer materials. Most primer cups utilize the same brass composition as the cartridge case, providing a balance of flexibility for deformation upon being struck by the firing pin and strength to withstand the primer explosion and discharge gas pressure. Among European manufacturers, the Berdan primer configuration is favored while American manufacturers preferentially utilize the Boxer primer configuration (Figure 1.2). The main difference between the two configurations is the location of the anvil within the primer cup. For the Berdan configuration, the anvil is built into the cartridge case and the primer combustion products pass to the propellant through two parallel flash holes. Within the Boxer configuration, a free-floating anvil is sealed within the primer cup and combustion products pass through a single, centrally

located flash hole. While both configurations achieve similar performance, Berdan primers are cheaper to manufacture although Boxer primers are simpler for reloading enthusiasts.

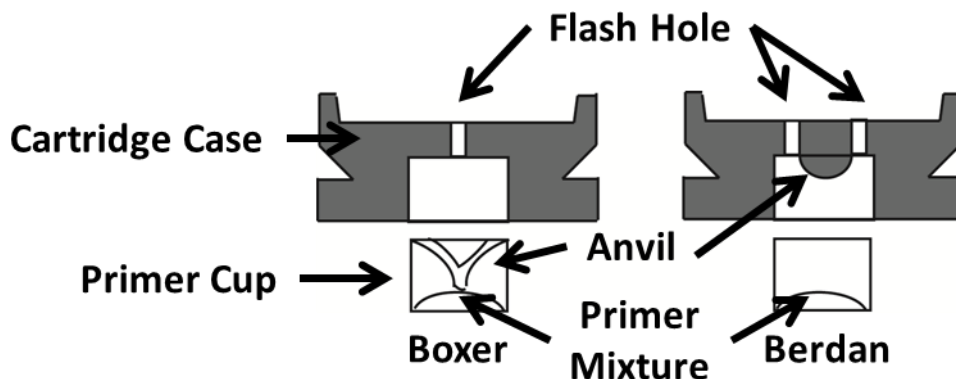


Figure 1.2: Boxer and Berdan primer differences

Primer mixtures for small firearms generally consist of an explosive, oxidizers, fuel, frictionators, sensitizers, and binders. Explosives include azides, fulminates, diazo compounds, and nitro or nitroso compounds such as lead azide, mercury fulminate, lead styphnate, trinitrotoluene, and pentaerythritol tetranitrate. The inclusion of oxidizers, such as barium nitrate, potassium chlorate, lead dioxide, and lead nitrate, ensure sufficient oxygen levels for full combustion of the fuel within the limited cap volume. Frictionators, such as ground glass or aluminum powder, and sensitizers, including tetracene, trinitrotoluene, and pentaerythritol tetranitrate, assist in transferring mechanical compression to detonate the explosive. Binders, such as gum Arabic, gum tragacanth, glue, dextrin, sodium alginate, rubber cement, and karaya gum, prevent settling and fix the concentration of individual components within the primer to avoid sensitivity issues.⁹

Propellants serve to provide large volumes of hot gases at highly controlled, predetermined rates to allow rapid and reproducible expulsion of the bullet from the ammunition. The combustion rate of a propellant must be balanced between high speeds, which would lead to detonation and severe damage to the weapon and operator and low speed, which would result in low projectile velocity. Careful design of the granule geometry along with the addition of surface coatings imparts control over the propellant burn rate. With few exceptions, modern smokeless propellants contain plasticized cellulose nitrate, commonly referred to as nitrocellulose, as the major oxidizing ingredient. Another high-energy plasticizer, commonly nitroglycerine, may be added to increase performance while fuel type plasticizers, such as phthalates, polyester adipate, and urethane, are used to improve physical and processing characteristics. The addition of stabilizers, such as diphenylamine, dinitrotoluene, centralites, or acardites limit the natural decomposition of nitrocellulose by reacting with the catalytic decomposition products to slow the decomposition rate. Inorganic additives, including chalk, graphite, potassium sulfate, potassium nitrate, and barium nitrate, may also be included to react with corrosive propellant decomposition products to prevent firearm damage from routine operation while also limiting muzzle flash and improving ignitability. When nitrocellulose is the only oxidizer present the propellant is said to be single base while the inclusion of a second oxidizer, such as nitroglycerin, classifies the propellant as double base. Modern smokeless powders produce little residue on combustion and generate less smoke than black powder. The major combustion products are nitrogen, carbon monoxide, carbon dioxide, hydrogen, and water vapor, with little contribution to inorganic GSR particles.⁹

Conventional bullets are non-spherical projectiles for use in rifled barrels and are designed for either penetration power or stopping power. Bullets may beunjacketed, partially jacketed, or full jacketed depending on the application. Unjacketed bullets composed of lead, are primarily confined to revolvers and other low-power firearms due to their relative fragility. For higher velocity applications, bullets must be at least partially jacketed with a stronger metal than lead to avoid deformation and detrimental stripping by rifled grooves which would lead to unreliable performance. In unjacketed and partially-jacketed bullets, the lead base is exposed to the hot propellant gases which cause erosion of lead particles and release into airborne emissions. In order to produce non-toxic ammunition, manufacturers must utilize a total metal-jacketed bullet to avoid lead release. Application of bullet jackets occurs though either electroplating or the pouring of molten lead into previously cast shells and crimping to seal. Gilding metal, a mixture of zinc in copper, is the most commonly utilized material for jacketing bullets.⁹

1.3 Forensic Gunshot Residue Detection

The detection of GSR commonly serves to assist in determining whether an individual recently fired a weapon, to designate a bullet entrance wound, or to estimate the distance from which a gun was fired from its target.³ While ammunitions contain both organic and inorganic components, only a small number of forensic laboratories attempt to classify organic components as they typically burn nearly to completion which renders detection challenging.

Typically, organic components are studied during wound entrance determination and firing distance estimation based on the use of color tests. Color tests provide a rapid indication of the potential presence and concentration of gunshot residue upon a surface. Beginning in 1933, the dermal nitrate or paraffin test was introduced in which a wax lift from a suspect's hand is exposed to an acidic nitro-group reactive molecule which produces a blue color upon exposure to smokeless powders and other nitro containing compounds.³ In the following years the Griess and Marshal tests, following similar chemical principles, have grown in popularity and still receive use today. Even with the introduction of the Lunge test, specific for nitrocellulose, color tests still lack the ability to discriminate between nitro-containing compounds resulting from the firing of a weapon and those present naturally in fertilizer, urine, tobacco and other common environmental sources.⁶

Generally, laboratories focus on the inorganic components present in GSR due to their persistence after firing and their potentially unique combined elemental profiles that can be used to discriminate ammunitions. In 1959, Harrison and Gilroy developed a color test for determining the presence of lead, barium, and antimony within a suspected GSR sample. First, swabs were moistened with dilute hydrochloric acid to collect GSR from suspected contaminated surfaces and hands. After drying, addition of triphenylmethylarsonium iodide would produce orange spots if antimony were present in the swab. After another drying, the addition of sodium rhodizonate resulted in red coloration in the presence of lead or barium. To confirm the presence of lead, the addition of dilute hydrochloric acid to the swab after rhodizonate testing changes the color from red to purple or blue while brown indicates the

presence of barium.¹⁰ While color tests can indicate the presence of a specific element, they suffer from low sensitivity and do not provide information about elemental concentration or the presence of other elements that do not react with the reagents utilized. To address these deficiencies, neutron activation analysis was first published as a method for determining antimony and barium within GSR in 1962.¹¹ While neutron activation analysis was the most sensitive technique available for metals at the time, the analysis of lead was not possible and access to nuclear reactors was necessary to generate the required neutrons. As a result, widespread forensic utilization of this technique was limited. In 1971, the first procedure for GSR analysis by atomic absorption spectroscopy was presented. This technique allowed for highly sensitive detection of lead but suffered from low sensitivity for barium and antimony.^{12,13} Additionally, in atomic absorption spectroscopy, elements are detected one at a time, making the detection of multiple elements in a sample time consuming. The use of inductively coupled plasma mass spectrometry (ICP-MS) was introduced for GSR determination in 1998 and allowed for superior detection limits and more rapid analysis as multiple elements can be detected simultaneously. Additionally, ICP-MS offers sufficient resolution to distinguish several isotopes for each element of interest.¹⁴ Several later studies demonstrated the ability of ICP-MS to distinguish between some types of ammunition based on elemental composition and isotopic profiles but the technique was not recommended for everyday case work since it was time consuming, destructive, and suffered from lead memory from previously fired ammunitions through the same firearm despite cleaning attempts.^{8,15,16} While these advanced

elemental analysis techniques provide some advantages over color testing, they are all bulk sampling methods and do not allow discrimination of GSR particles on an individual basis.

The most commonly utilized instrument for GSR analysis in forensic examinations is the scanning electron microscope (SEM) with an attached energy dispersive X-ray spectroscopy (EDS) detector. While ICP-MS and other bulk techniques have low limits of detection for elements of interest in GSR analysis, SEM-EDS allows for both elemental information as well as morphological characterization on a particle-by-particle basis. The SEM-EDS system was first explored for forensic GSR analysis in 1968 allowing for magnifications up to 100,000x with 200 times the depth of field provided by standard optical microscopy.¹⁷ Most importantly, the SEM-EDS system analyzes single particles in a nondestructive manner allowing for high specificity well beyond the capabilities of bulk analysis techniques like ICP-MS. To begin analysis, items such as hands or clothing where GSR may be present are sampled using either a tape lift procedure or repeated exposure to a conductive carbon adhesive surface suitable for analysis by SEM-EDS. Oftentimes, laboratories may also wish to apply a thin carbon coating of several nanometers in thickness atop the adhesive surface to ensure conductivity within the SEM-EDS system. Once prepared, the sample is inserted into the instrument and must be searched for the presence of particles, which can be a laborious task. Fortunately, the development of automated search programs now allows analysts to merely confirm findings suggested by the software rather than invest their time conducting a manual search.¹⁸⁻²¹ Once potential GSR particles are located, the SEM is focused at a specified magnification and both the particle morphology and elemental composition are recorded. Spherical particles consisting solely of

lead-barium-antimony, barium-antimony, or lead-barium-calcium-silicon-tin are considered unique to the explosion of an ammunition primer.^{22,23} Many other particle compositions are also often discovered and their presence is considered indicative of GSR but they may also result from environmental sources and thus require analysis by a trained expert on a case-by-case basis to determine the most likely source of the particles.³

1.4 Environmental Sources of Gunshot Residue Like Particles

In order for the identification of GSR components to be of evidentiary value, the source of the components must be determined with reasonable certainty. This requirement may be another reason for the lack of utilization of organic components of GSR as these components are present in the environment. For example, a common ammunition stabilizer, diphenylamine, is also used in solid rocket fuels, pesticides, dyes, and pharmaceuticals.²⁴ Diphenylamine has even been detected on apple skins, tires, and clothing.²⁵

Inorganic components of GSR are also present naturally in the environment, or can be produced through activities other than the discharge of a firearm. In 1979, Wolten et al. identified a critical group of occupations with the greatest potential for exposure to particles similar to GSR. After sampling employees, particles indicative of GSR were located on individuals working with stud guns, as automotive brake mechanics, and as lead acid battery assemblers.²⁶ Further studies corroborated these initial findings resulting in a recommendation

to move from a strict particle classification system to a case-by-case basis, taking into account any known details of a particular case.^{22,23,27} Other researchers have explored the potential for fireworks and incendiary devices to produce particles consistent with GSR and found that particles consisting of barium-antimony or lead-barium-antimony, which were previously thought to be unique to GSR, were produced after ignition of some commercial and residential fireworks.²⁸ While the composition of these environmental particles could be confused with GSR, the morphology of the particles was generally different. Based on the high likelihood of environmental contamination, modern analysis dictates the only reliable particle which can be attributed to GSR must have ideal spherical morphology with a diameter typically between 0.5-5 μm and an elemental composition consistent with GSR. Likewise, any evidence presented without providing ammunition to serve as a comparison from the suspect should be treated with caution.²⁹

The introduction of non-toxic ammunition to the marketplace provides further challenges for distinguishing between GSR and environmental particles. Sintox ammunition was previously studied and found to contain particles of titanium and zinc with spherical morphologies.³⁰ Only the unique spherical morphology of these particles resulting from the high pressure and temperature produced upon discharging a firearm allowed them to be distinguished from similar non-spherical particles common to paints. Similarly, CCI Blazer ammunition was found to contain primarily strontium, a known major component of road flares and fireworks.³¹ While non-toxic ammunition generally produced less spherical particles than

traditional ammunition, MagTech Cleanrange only produced irregularly shaped particles, thus further complicating GSR analysis.³² With the continuing addition of non-toxic ammunition to the market, further analysis of environmental sources of similar particles must be completed to assign appropriate evidentiary value in cases where non-toxic ammunition is used.⁴

1.5 Research Objectives

The variable and changing nature of commercially-available, non-toxic ammunition compositions provides serious evidentiary reliability questions for the forensic science community. Previous researchers utilized SEM-EDS to address some aspects of understanding the particles produced by non-toxic ammunition, as well as the potential for environmental particle similarity. However, the lack of published elemental profiles for all commercially available non-toxic ammunition as well as limited statistical assessment of the data to discriminate among brands and from environmental sources demonstrate a need for further study. Based on these challenges, the goals of this project were:

- To determine the elemental composition of a variety of commercially available non-toxic ammunition, as well as road flares, and
- To assess principal components analysis procedures to discriminate non-toxic ammunition from different manufacturers, as well as from road flares based on element compositions

The results of this study will benefit trace evidence and firearms analysts tasked with characterizing non-toxic ammunition. The elemental profiles generated will allow for comparison with suspected GSR particles inconsistent with previously published ammunition in cases where limited knowledge of the weapon exists. The evaluation of statistical procedures for distinguishing ammunition from different manufacturers as well as from environmental sources will allow for statistical confidence in the uniqueness of a particle, thus providing evidentiary value to a discipline still lacking known error rates.

REFERENCES

REFERENCES

- (1) Landrigan, P. J.; McKinney, A. S.; Hopkins, L. C.; Rhodes, W. W.; Price, W. A.; Cox, D. H. *Journal of the American Medical Association* **1975**, 234, 394.
- (2) Robbins, S. K.; Blehm, K. D.; Buchan, R. M. *Applied Occupational and Environmental Hygiene* **1990**, 5, 435.
- (3) Romolo, F. S.; Margot, P. *Forensic Science International* **2001**, 119, 195.
- (4) Oommen, Z.; Pierce, S. M. *Journal of Forensic Sciences* **2006**, 51, 509.
- (5) Schwoeble, A. J.; Exline, D. L. *Current Methods in Forensic Gunshot Residue Analysis*; CRC Press: Boca Raton, FL, USA, 2000.
- (6) Dalby, O.; Butler, D.; Birkett, J. W. *Journal of Forensic Sciences* **2010**, 55, 924.
- (7) Edwards, H. T.; Gatsonis, C.; Berger, M. A.; Cecil, J. S.; Bonner-Denton, M.; Fierro, M. F.; Kafadar, K.; Marone, P. M.; Mearns, G. S.; Murch, R. S.; Robertson, C.; Schechter, M. E.; Shaler, R.; Siegel, J. A.; Srihari, S. N.; Wiederhorn, S. M.; Zumwalt, R. E. *Strengthening Forensic Science in the United States: A Path Forward*; 1st ed.; National Academies Press: Washington, D.C., 2009.
- (8) Steffen, S.; Otto, M.; Niewoehner, L.; Barth, M.; Brožek-Mucha, Z.; Biegstraaten, J.; Horváth, R. *Spectrochimica Acta Part B: Atomic Spectroscopy* **2007**, 62, 1028.
- (9) Wallace, J. S. *Chemical Analysis of Firearms, Ammunition, and Gunshot Residue*; CRC Press: Boca Raton, FL, 2008.
- (10) Harrison, H. C.; Gilroy, R. *Journal of Forensic Sciences* **1959**, 4, 184.
- (11) Ruch, R. R.; Buchanan, J. D.; Guinn, V. P.; Bellanca, S. C.; Pinker, R. H. *Journal of Forensic Sciences* **1964**, 9, 119.

- (12) Krishnan, S. S. *Journal of Forensic Sciences* **1971**, 16, 144.
- (13) Stone, I. C.; Petty, C. S. *Journal of Forensic Sciences* **1974**, 19, 784.
- (14) Koons, R. D. *Journal of Forensic Sciences* **1998**, 43, 748.
- (15) Zeichner, A.; Ehrlich, S.; Shoshani, E.; Halicz, L. *Forensic Science International* **2006**, 158, 52.
- (16) Sarkis, J. E. S.; Neto, O. N.; Viebig, S.; Durrant, S. F. *Forensic Science International* **2007**, 172, 63.
- (17) Heard, B. J. *Handbook of Firearms and Ballistics*; Wiley: Chichester, 1997.
- (18) Kee, T. G.; Beck, C. *Journal of the Forensic Science Society* **1987**, 27, 321.
- (19) Tillman, L. *Journal of Forensic Sciences* **1987**, 32, 62.
- (20) White, R. S.; Owens, D. A. *Journal of Forensic Sciences* **1987**, 32, 1595.
- (21) Germani, M. S. *Journal of Forensic Sciences* **1991**, 36, 331.
- (22) Wallace, J. S.; McQuillan, J. *Journal of the Forensic Science Society* **1984**, 24, 495.
- (23) Zeichner, A.; Levin, N. *Journal of Forensic Sciences* **1997**, 42, 1027.
- (24) Hawley, G. G. *The Condensed Chemical Dictionary*; 10th edition ed.; Van Nostrand-Reinhold: New York, NY, 1981.
- (25) Lloyd, J. B. F. *Analytical Chemistry* **1987**, 59, 1401.
- (26) Wolten, G. M.; Nesbitt, R. S.; Calloway, A. R.; Loper, G. L. *Journal of Forensic Sciences* **1979**, 24, 423.

- (27) Garofano, L.; Capra, M.; Ferrari, F.; Bizzaro, G. P.; Di Tullio, D.; M., D. O.; Ghitti, A. *Forensic Science International* **1999**, *103*, 1.
- (28) Mosher, P. V.; McVicar, M. J.; Randall, E. D.; Sild, E. D. *Canadian Society of Forensic Science* **1998**, *31*, 157.
- (29) Torre, C.; Mattutino, G.; Vasino, V.; Robino, C. *Journal of Forensic Sciences* **2002**, *47*, 494.
- (30) Gunaratnam, L.; Himberg, K. *Journal of Forensic Sciences* **1994**, *39*, 532.
- (31) Harris, A. *Journal of Forensic Sciences* **1995**, *40*, 27.
- (32) Martiny, A.; Campos, A. P. C.; Sader, M. S.; Pinto, M. A. L. *Forensic Science International* **2008**, *177*, e9.

CHAPTER 2: THEORY

2.1 Gunshot Residue Formation

As the primer ignites causing the propellant to burn within a round of ammunition, temperatures exceeding 3,000 °C and pressures above 3,000 atmospheres develop within the firearm.¹ Under these extreme conditions, both organic and inorganic components of the primer and propellant vaporize within a few milliseconds. The unique composition of gunshot residue (GSR) results from the vaporization of lead, barium, and antimony (present in the primer) among other components as each element is subjected to temperatures above their boiling points of 1,620 °C, 1,140 °C, and 1,380 °C, respectively. As the temperature of the vaporized mixture decreases, the inorganic vapors condense into liquid droplets and deposit onto solid surfaces. This rapid vaporization and condensation process likely occurs within the primer before the propellant even ignites.² Therefore, particles may form from condensation of products resulting from primer combustion, propellant burning, or both.

Previous researchers suggest classifying GSR as arising from either the primer or the bullet based on its elemental composition.³ GSR resulting solely from primer combustion likely contains metal oxides, sulfides, and salts due to the presence of these components as compounds within the primer mixture. Despite the extreme oxidative conditions present causing the vaporization of the compounds, degradation does not occur and thus the production of particles consisting of pure elements is unreasonable. For particles arising from

the bullet, pure metals are originally present in the bullet composition and therefore resulting particles may be elementally pure.³

Further research classified the formation of inorganic GSR particles resulting from a common primer containing a mixture of lead styphnate, barium nitrate, and antimony trisulfate into three distinct categories. The first category includes the particles most commonly detected on the hands of a person after discharging a firearm. These particles, which account for 68% of observed particles, are characterized as small, spherical particles that may have small bulges on their surfaces. The bulges are typically composed of a single element which may not include lead, barium, or antimony. The bulges are thought to be the result of interactions between solidifying particles and smaller molten droplets. The spherical particles, which typically have diameters ranging from 2-10 μm , generally contain a uniform mixture of lead, barium, and antimony. Due to their small size, these particles likely form prior to propellant burning and travel quickly along the propellant detonation front so as to be unaffected by the propellant mixture. The second category comprises 25% of observed particles and consists of irregularly shaped particles with a heterogeneous distribution of lead, barium, and antimony. These particles also commonly contain hollow cores which indicate the presence of a disturbance during formation. This disturbance likely occurs during the detonation of the propellant mixture as the increased particle diameter compared to the first category indicates category two particles spend more time within the casing allowing for the higher particle size growth. The final category of particles consists of a lead coating surrounding a homogeneous core mixture of barium and antimony. These particles likely result from the exposure of solidifying barium-

antimony particles to lead vapors present from the vaporization of the bullet during the propellant combustion. Category three particles are also larger than those in category one indicating their slow exit from the combustion mixture similar to category two particles.²

While most leaded and lead-free GSR particles observed are roughly spheroidal in morphology, irregular particles are also observed similar to category two primer particles. Irregularity may in fact result from the deposition of molten GSR onto solid surfaces. Previous research observed particles splattered or flattened on surfaces after impact causing severe deformation especially at target distances between 20 and 30 cm. At short target distances, particles larger than 2 μm are still molten upon striking the target leading to shattering or adhesion to the surface upon contact.⁴ Lead-free GSR should likely behave in the same way since only the composition of the primers is different. Therefore, while the presence of spherical particles is useful for distinguishing GSR from environmental particles of similar composition, their absence should not be used as proof a weapon was not recently fired. Although unlikely, it remains possible that all particles recovered in a suspected shooting situation could be irregular, especially at short distances directed to a solid surface. Additionally, little research is available on the differences in GSR formation from lead-free ammunition and thus the ratio of spherical to irregular particles is yet unknown.

2.2 Scanning Electron Microscopy/Energy Dispersive X-ray Spectroscopy

The use of scanning electron microscopy (SEM) allows for resolution of particles and features down to single nanometer length scales, well beyond the capabilities of optical microscopy. While optical microscopy focuses a column of light onto the sample through a series of lenses, SEM utilizes a powerful beam of electrons directed at the sample at much shorter wavelengths than visible light allowing for the enhanced resolution. In addition to high resolution, SEM also offers a long depth of field allowing for observation of spatial features of samples at increased depths. Meanwhile, the energy dispersive X-ray (EDS) system determines the elemental composition of samples based on the emission of characteristic X-ray wavelengths arising from the interaction of electrons with atoms in the sample surface.⁵

The basic design of a modern SEM (Figure 2.1) includes an electron source, one or more sets of condenser lenses, an objective lens, and several detectors. The electron source may be operated in either cold or hot mode to produce electrons. In hot operation, an electron source such as a tungsten filament or a lanthanum hexaboride cathode is heated until electrons are released thermionically. In cold operation, a field emission electron source produces electrons through tunneling at room temperature, relying on a high voltage drop between the field emission tip and the electron chamber while under high vacuum. In both hot or cold modes, the broad source electrons generated are then focused to an adjustable spot size utilizing electromagnetic condensing lenses. After condensing the beam to the desired spot size, the objective lens directs the beam to raster the sample surface providing illumination of the sample. Upon the beam striking the sample, electrons are released in the form of secondary

electrons from the ionization of the surface or in the form of backscattered electrons from elastic beam-surface interactions. The secondary electrons and backscattered electrons are collected by two separate detectors. Additionally, the removal of inner shell electrons from atoms in the sample causes a release of energy in the form of an X-ray of a characteristic wavelength, which may be detected and quantified by the EDS detector.⁵

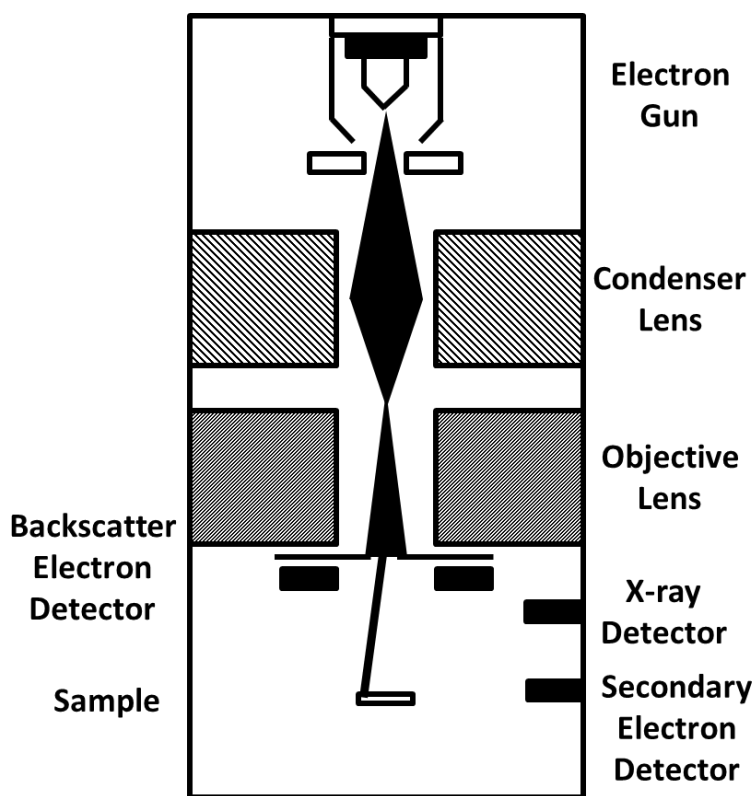


Figure 2.1: Schematic of a SEM-EDS system

To prepare samples for SEM-EDS analysis, the surface must be relatively conductive to avoid the buildup of excess negative charge due to the high beam current utilized in SEM. Typical beam currents for SEM range from 0.2-40 nA allowing magnifications of up to 500,000

times with a spot size ranging from 0.4-5 nm. In order to increase the conductivity of non-conductive samples, many samples receive a 10-30 nm coating of gold or carbon particles deposited through a sputter coating instrument. To sputter a layer of gold onto a sample, the sample is first placed inside a sealed chamber within the sputter coating instrument. The pressure of the chamber is then reduced and flushed with an inert gas such as argon. Once a stable vacuum pressure is reached, argon ions are driven towards a gold target at high velocities under the control of an applied electric field. As the argon strikes the gold target, gold atoms are released, coating the sample surface and increasing conductivity. The deposition of carbon works in a similar manner except the carbon fragments are generated through the heating of a carbon filament to extreme temperatures under vacuum.⁵

Samples are introduced to the SEM through a series of vacuum lock chambers allowing a gradual reduction in pressure surrounding the sample. This is necessary to pass the sample into the vacuum environment accessible by the electron beam. Once the sample is positioned within the SEM stage, the electronic beam is switched on and the secondary electron detector is activated allowing for topographical imaging of the sample. Secondary electrons are detected using an Everhart-Thornley detector which collects the negative secondary electrons emitted from samples using a collector at a high positive potential. Once the secondary electrons strike the collector, photons of light are released and enter a photomultiplier tube where the photons are amplified as electrons for image processing by the software. The sample stage moves either manually or through computer control allowing imaging of the entire sample surface. Once operational, the backscattered electron detector may be switched on providing contrast in the

image based on the average atomic number of elements within the sample bulk. Backscattered electrons are detected through use of a Robinson or semiconductor detector placed directly above the sample to capture the high energy backscattered electrons from the sample.⁶

Likewise, the EDS detector can run simultaneously to provide detailed information about the elemental composition of a surface with a minimal resolution of several micrometers. X-rays first must pass through a collimator near the sample which permits passage of radiation resulting from a specified angle from the sample. The X-rays then pass through a beryllium window which serves to protect the detector crystal from vapors in the sample chamber which would condense on the liquid nitrogen cooled crystal. As the X-rays strike the detector crystal, which is comprised of a silicon wafer coated in lithium, short voltage pulses result corresponding to the energy of the incident radiation. The pulses then pass through the field-effect transistor, which amplifies the pulses for analysis by the system software to visually display the detected elements in the form of an X-ray spectrum. Due to the quantized nature of atomic shells, the energy of the X-ray for each element has a characteristic energy used for identification of elements present in a sample.

2.3 Principal Components Analysis

Principal components analysis (PCA) assesses the correlation between variables in a data set and produces a visual representation of differences in the variance between samples within the data set. PCA assumes that complex multivariate data, such as energy spectra, chromatograms, and mass spectra, often contain underlying correlated variables based on

coupling effects of chemical composition or structure.⁷ Through identification of these correlated variables, the dimensionality of the data set may be reduced while maintaining the underlying structure of the data.⁸ PCA determines orthogonal, linear combinations of the correlated variables which incorporate the greatest amount of variance to form a new set of uncorrelated variables. The original multivariate data are projected into the resulting lower dimensional plots for visual association and discrimination of samples.⁷

The linear combinations of correlated variables are known as eigenvectors and are classified as principal components (PC) in order of decreasing eigenvalues. The eigenvalues associated with each eigenvector indicate the percent of variance accounted for by the eigenvector. Hence, PC1 explains the highest percentage of the variance in the data set, PC2, which is orthogonal to PC1, explains the next highest percentage variance, and so on, all the way down to the least informative component described by PC n where n is the smaller value for the total number of samples or variables. In PCA, typically only a few (~3) PCs are necessary to describe nearly all of the variance within a data set. Therefore, the data can be represented as a two or three dimensional scatter plot without compromising the underlying structure.⁹ In this way, minor differences among samples within a data set sharing high similarity are elucidated from the noise allowing for more efficient association and discrimination of samples.

PCA commonly only requires the first two PC to describe a meaningful (>70%) amount of the variance for samples with reasonable correlation.⁹ In these cases, samples are plotted on an XY scatter plot with the first two PCs as the X and Y axes in what is known as a scores plot.

Samples that are highly correlated, such as those with chemically similar compositions, will position near one another and move away from the positioning of samples with chemically dissimilar compositions. This visual clustering in the scores plot allows conclusions to be drawn about how each sample relates to the others. The positioning of samples in the scores plot can be explained with reference to the loadings plots that are also generated in PCA. These plots show which variables in the samples are contributing to the variance described by each PC. Directly correlated variables are weighted similarly in sign (either positively or negatively) while inversely correlated components are weighted opposite in sign within the loadings plot. The magnitude of each variable in the loadings plot is directly related to its contribution to the variance described by the PC. Samples comprised primarily of variables which greatly contribute to the overall variance will be positioned at further distances from the origin of the scores plot than those lacking such variables.

PCA provides an interesting method of associating and discriminating GSR evidence from known standards and environmental sources, respectively. As a multivariate procedure, PCA considers all variables simultaneously, rather than individually as is the case with univariate statistical procedures. Hence, discrimination of apparently similar samples may be possible based on the relative differences in abundance of all of the elements present. Such differences are potentially not apparent using univariate statistical procedures, in which only relative differences in abundance of one element at a time can be considered. The discriminating ability of PCA, coupled with further statistical testing to assign confidence values, should enhance the forensic significance of GSR comparisons in evidentiary situations. Additionally, PCA also indicates which elements in the GSR compositions contribute the most to the discrimination of

the samples to further explore the effect slight compositional differences hold over the ability to discriminate samples based on elemental composition.

REFERENCES

REFERENCES

- (1) Wallace, J. S. *Chemical Analysis of Firearms, Ammunition, and Gunshot Residue*; CRC Press: Boca Raton, FL, 2008.
- (2) Basu, S. *Journal of Forensic Sciences* **1982**, 27, 72.
- (3) Wolten, G. M.; Nesbitt, R. S. *Journal of Forensic Sciences* **1980**, 25, 533.
- (4) Burnett, B. *Journal of Forensic Sciences* **1989**, 34, 808.
- (5) Flegler, S. L.; Heckman, J. W.; Klomparens, K. L. *Scanning and Transmission Electron Microscopy An Introduction*; W.H. Freeman and Company: New York, NY, 1993.
- (6) Robinson, B. W.; Nickel, E. H. *American Mineralogist* **1983**, 68, 840.
- (7) *Forensic Science on the Cutting Edge: New Methods for Trace Evidence Analysis*; Blackledge, R. D., Ed.; John Wiley & Sons, Inc.: Hoboken, NJ, 2007.
- (8) Hotelling, H. *Journal of Educational Psychology* **1933**, 10, 69.
- (9) Varmuza, K.; Filzmoser, P. *Introduction to Multivariate Statistical Analysis in Chemometrics*; CRC Press: Boca Raton, FL, 2009.

CHAPTER 3: MATERIALS AND METHODS

3.1 Experimental Design and Sample Collection

3.1.1 Primer Study

Six different commercially available 9 mm lead-free ammunitions were purchased from local stores and online suppliers. Purchased ammunition consisted of Remington UMC Leadless 9 mm Luger 147 grain Flat Nose Enclosed Base (Rem) (Lonoke, AR), Winchester Super Clean NT 9 mm Luger 105 grain Jacketed Soft Point (WinSC) (East Alton, IL), Winchester WinClean 9 mm Luger 147 grain Brass Enclosed Base (WinCI) (East Alton, IL), Magtech Cleanrange 9 mm Luger 115 grain Fully Encapsulated Bullet (Mag) (Lino Lakes, MN), CCI Blazer Clean-Fire 9 mm Luger 124 grain Totally Metal Jacketed (CCI), and Sellier & Bellot Nontox 9 mm Luger 115 grain Totally Full Metal Jacketed (S&B) (Lewiston, ID). Under the supervision of the Michigan State Police Bridgeport Laboratory, five rounds of ammunition of each type were disassembled using a kinetic bullet pulling system to dislodge the bullet from the shell casing. With the bullet out of the way, all propellant powder was removed from each casing leaving only the intact sealed primer cup and shell case behind. A Glock 17 slide and barrel were taken from a decommissioned firearm and cut to remove the length of the barrel leaving only the portion required to hold the cartridge case containing the primer (Figure 3.1). The barrel length was removed to avoid any contamination from the barrel in primer composition studies.



Figure 3.1: Glock 17 slide and barrel after removing barrel length (above) compared to unmodified components from another Glock 17 (below).

Primers contained in their cartridge cases (five samples for each of the ammunition types) were placed in the shortened barrel chamber and aimed downrange towards two 12 mm adhesive carbon tabs (Ted Pella Inc., Redding, CA) suitable for direct SEM imaging (Figure 3.2). The carbon tabs were placed 15 cm downrange from the barrel aligned perpendicular to the path of ejected primer particles similar to systems used by previous researchers.^{1,2} Perpendicular placement of the tabs attempted to achieve maximum particle recovery through exposing the highest surface area possible to discharged particles. Each of the five rounds of ammunition from each of the six boxes was hand fired by pulling back the firing pin present in the slide and allowing it to strike the primer cup seated within the chamber. After each firing, two new conductive tabs were placed in the holder in preparation to collect particles from the

next sample. Each set of conductive tabs removed was stored in sealed plastic petri dishes until analysis by scanning electron microscopy with energy dispersive X-ray spectroscopy (SEM-EDS) to avoid extraneous particle contamination. After each set of five primers from a box was completed, the exhaust fan was switched on in the range to remove any remaining particles floating in the air and avoid cross-contamination between samples. During the entire time the firing range was in operation for this study, separate conductive tabs were left exposed to the air to detect any particles present as a control experiment to help identify the possibility of particle carryover or contamination from the range.

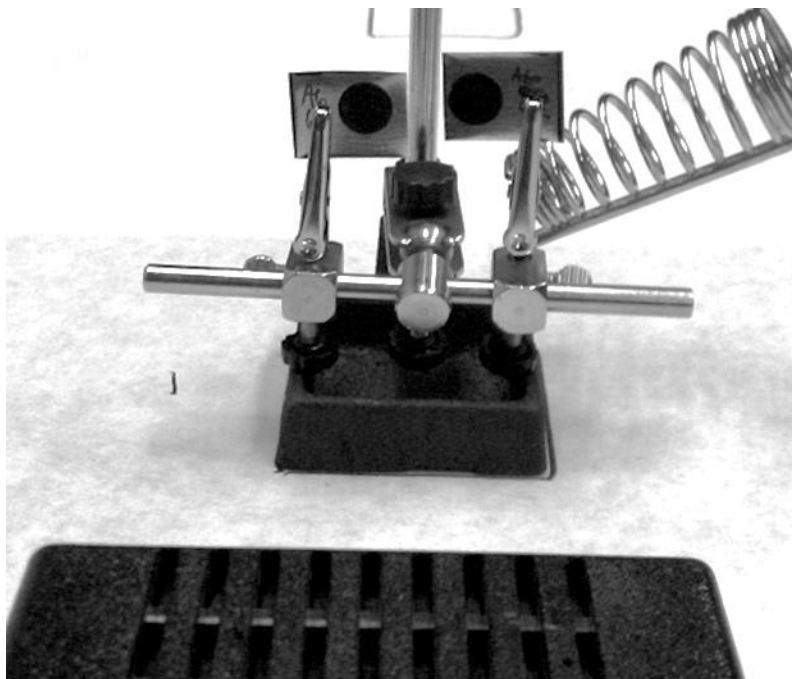


Figure 3.2: Dual conductive carbon tab placement 15 cm downrange perpendicular to particle trajectory during primer composition studies.

3.1.2 Intact Ammunition Study

Once again, five rounds of ammunition from each of the six boxes purchased were used for the intact ammunition study. All were fired by Michigan State Police Bridgeport Laboratory personnel downrange using a Ruger KP95DC 9mm pistol (Sturm, Ruger & Co., Southport, CT) (Figure 3.3) supported on a firing stand (Figure 3.4). Two 12 mm conductive carbon tabs (Ted Pella Inc.) were placed 15 cm downrange with one parallel and one perpendicular to the bullet trajectory (Figure 3.5). An additional carbon tab was placed 10 cm downrange parallel to the bullet trajectory as well. Carbon tab placement parallel to bullet trajectory attempted to ensure recovered particles were present on the surface of the adhesive rather than buried within it due to the possibility that extra force present from the propellant would lead to discharged particle velocities high enough to penetrate deep into the adhesive coatings. Particles deep within adhesive films would be more challenging to analyze and determine a representative elemental composition. After each fired shot, all three carbon tabs were placed into a sealed petri dish to avoid contamination and new tabs were positioned prior to the next shot. After all five firings were completed for each ammunition, the exhaust fan over the range was switched on to remove any remaining airborne GSR particles. Again, during the entire time the firing range was in operation for this study, separate conductive tabs were left exposed to the air to detect any particles present as a control experiment to help identify the possibility of particle carryover or contamination from the range.



Figure 3.3: Ruger KP95DC 9mm pistol supported on firing stand for intact ammunition studies. For interpretation of the references to color in this and all other figures, the reader is referred to the electronic version of this thesis.

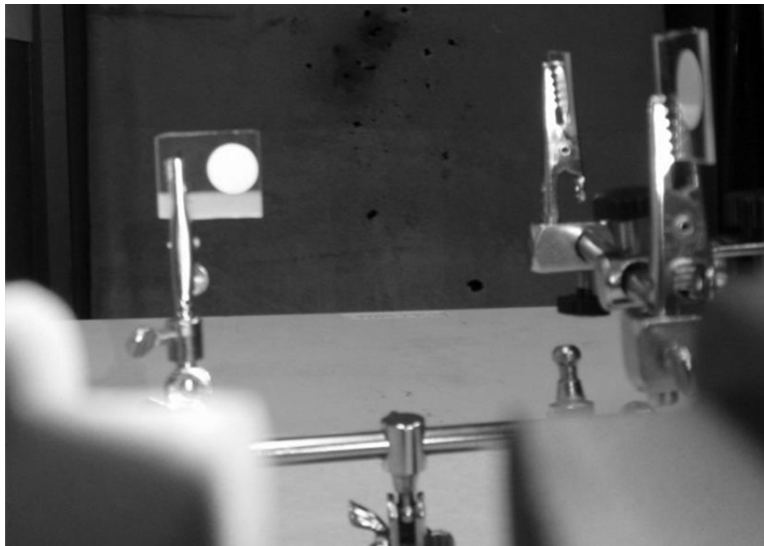


Figure 3.4: Barrel view downrange through adhesive tabs documenting the bullet trajectory during intact ammunition composition studies.

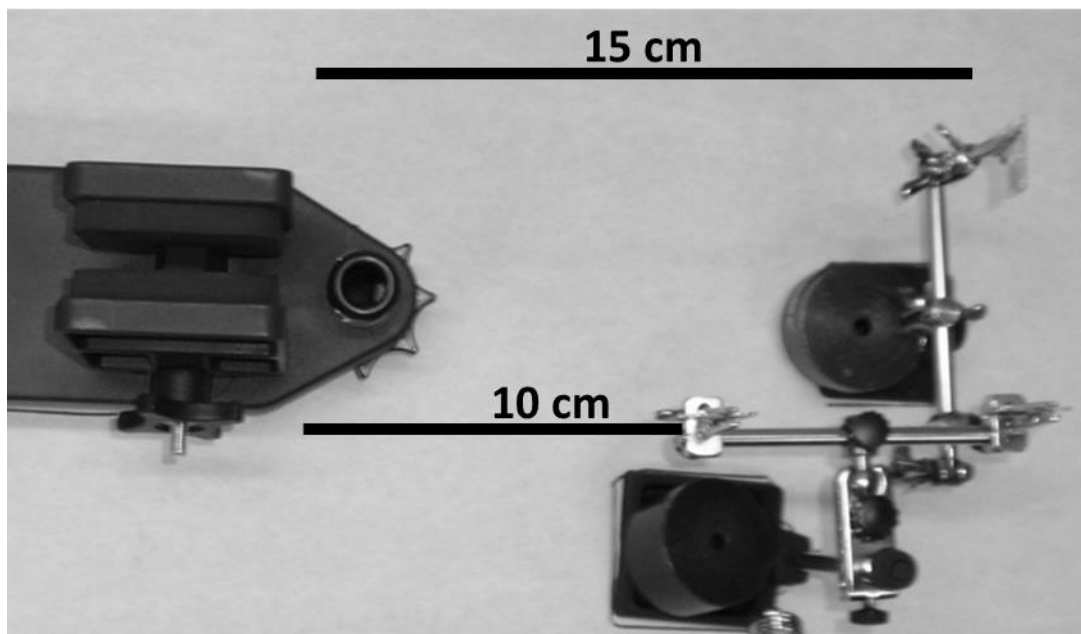


Figure 3.5: Dual conductive carbon tab placement 15 cm downrange (1 parallel, 1 perpendicular) along with a third tab placed 10 cm downrange parallel to bullet trajectory during intact ammunition composition studies.

3.1.3 Road Safety Flare Study

After searching the local area for road flare options, it quickly became evident only one manufacturer produces a majority of road flares available domestically. Ideally this study would have been able to explore differences between flare manufacturers but Orion Safety Products dominates the market. Therefore, an Orion flare (Orion Safety Products, Easton, MD) was purchased from a local vendor to explore whether flare ignition and burning produces particles similar to those recovered from non-toxic ammunitions. The flare was burned outdoors in an open fire-pit and multiple carbon tabs (Ted Pella Inc.) were held 10 cm above the burning flare for 1 minute to capture any discharged particles. After exposure to the burning flare, all samples were stored in a petri dish awaiting analysis by SEM-EDS.

3.2 SEM-EDS Analysis of GSR Particles

All carbon tab samples were analyzed as recovered without any further processing or surface treatments. SEM-EDS analysis utilized a Hitachi S4700-II field emission SEM (Hitachi High Technologies America, Schaumburg, IL) equipped with a EDAX Phoenix EDS system (EDAX, Mahwah, NJ) containing a Sapphire Si(Li) detector for determining elemental composition. Samples were manually scanned in secondary electron mode at 500x magnification using an accelerating voltage of 20 keV at a working distance of 12 mm. Most forensic work utilizes back-scattered electrons to search for GSR due to increased contrast arising from elemental differences between the GSR and support. However, the use of back-scattered electron mode was not possible due to the placement of the EDS detector between the sample and the back-scatter detector in the sample chamber as the SEM-EDS was currently set up.

Samples were scanned manually to locate suspected GSR particles based on the observation of small (1-50 μm), spherical particles. Once located, the EDS system was directed to obtain an elemental profile of the region containing the particle using a live time of 8 seconds (Figure 3.6). If the particle was found to differ in composition from the background, the visible area was labeled as a region of interest and all other potential GSR particles within view were analyzed by EDS to record their individual elemental compositions. Each particle characterized was recorded with any necessary notes in a file corresponding to each day's analysis. Each sample (primer only, intact ammunition, and road flare) was searched for particles in a serpentine pattern until a total of 30 regions of interest were designated. Thirty regions of interest were deemed suitable for further statistical analysis of the data.

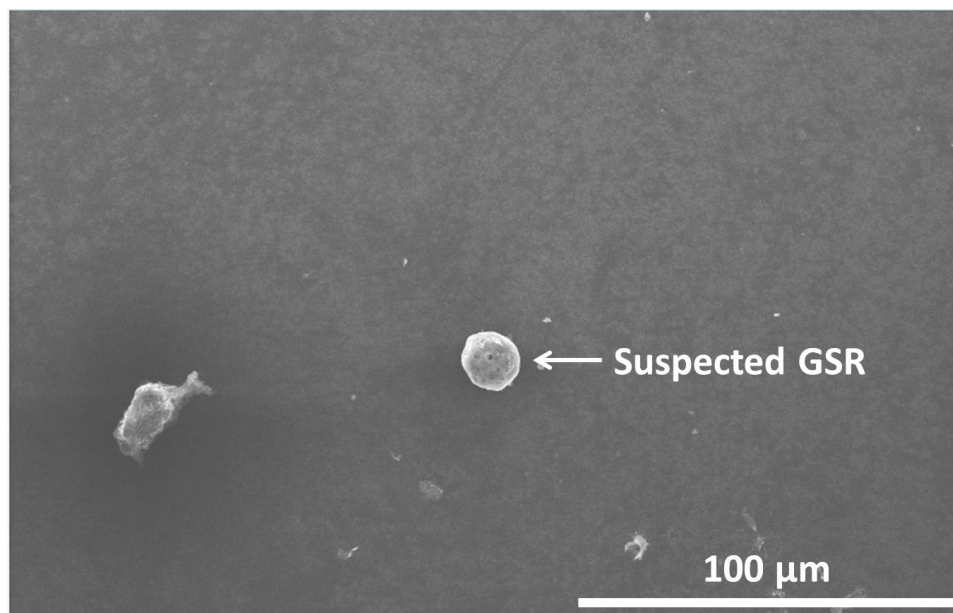


Figure 3.6: Suspected GSR particle located during manual SEM-EDS search at 500x magnification with a 20 keV accelerating voltage in secondary electron imaging mode.

3.3 Data Processing

Resulting EDS spectra were individually opened in the EDAX Spectrum Viewer software (version 4.0, EDAX) and the counts for each energy channel were exported to Microsoft Excel (2010 version, Microsoft Corp., Redmond, WA) for further data processing. As can be seen in the representative EDS spectrum shown in Figure 3.7, the most significant X-ray emission peaks detected in this study were positioned at energies less than 5 keV. To avoid incorporating small differences from noise and baseline fluctuations into the subsequent statistical analysis, all EDS spectra were truncated at 5 keV. Additionally, because most particle sizes are below the resolution of the EDS system, nearly every spectra collected includes carbon and oxygen peaks resulting from the carbon tab. While carbon and oxygen may be contained within GSR particles, EDS is unable to distinguish the source of each elemental contribution. Hence, carbon and

oxygen were excluded as elements of interest by beginning each spectrum at 0.7 keV as shown in Figure 3.8.

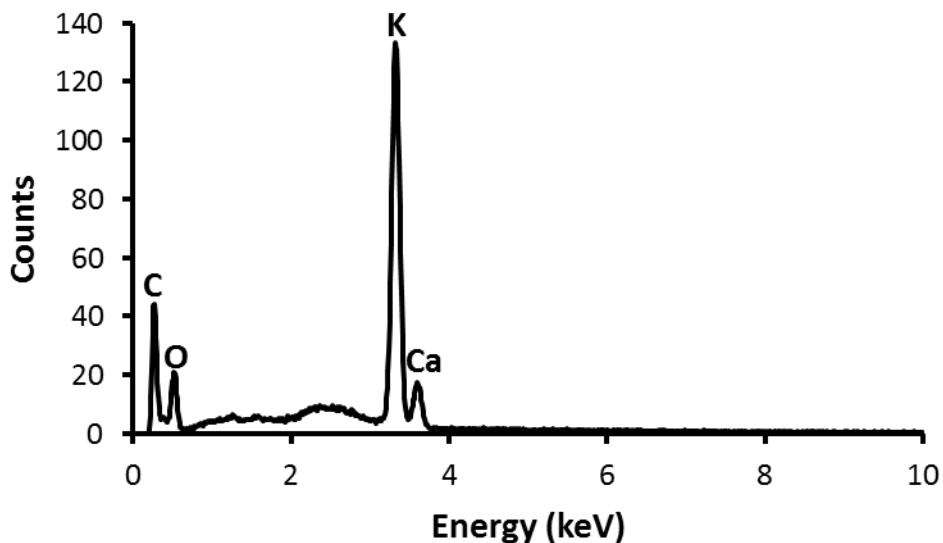


Figure 3.7: Representative EDS spectrum for a suspected GSR particle showing elemental contributions from carbon, oxygen, potassium, and calcium.

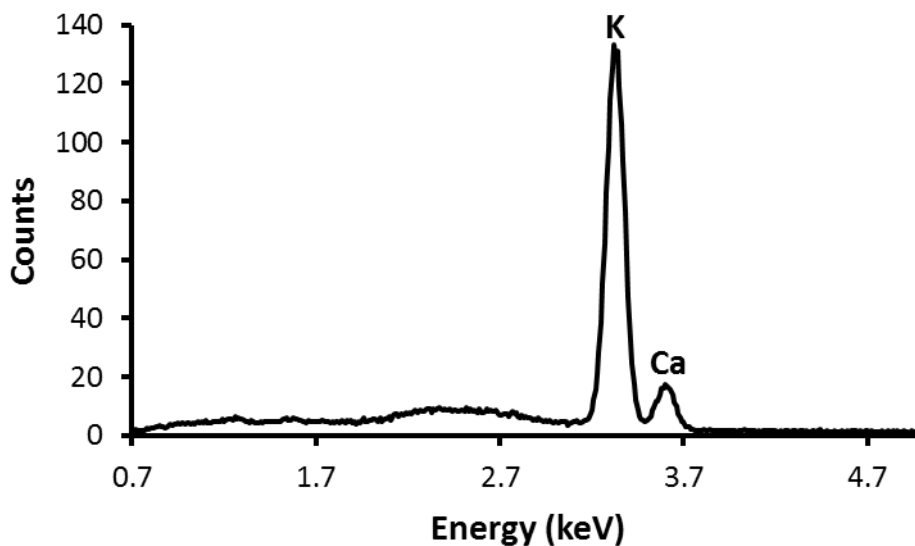


Figure 3.8: Representative EDS spectrum after removing background elemental contributions and empty energy channels.

After truncation, a single Excel file was generated containing all spectra for a single firing. This was repeated for all five firings of the isolated primers and the intact ammunition for all ammunition types, producing 60 total files. Since copper was a common component of all ammunitions tested either as a bullet jacket material or in the cartridge case, spectra consisting primarily of copper were excluded from further study. As copper particles are not unique to any of the ammunitions, removal of these spectra was necessary to improve the chance that discrimination may be possible based on manufacturer.

3.4 Principal Components Analysis of EDS Spectra

Upon looking over the particles collected for each firing of a particular ammunition, it was evident particles with a wide variety of compositions resulted from a single firing event. This high variability would complicate PCA analysis by introducing large amounts of variance within a single sample and would likely prevent clear differentiation of samples from different manufacturers. In order to overcome this high degree of variance among samples, the EDS spectra for all particles observed during a single firing event were averaged. For each firing, the number of particles documented in this study ranged from 12 up to 100 with an average of 50 particles for all replicates. Once all the particles were averaged for each firing event, the average spectra for the five firings from the same ammunition type were maximum peak normalized (Figure 3.9). For maximum peak normalization, every energy count value in each spectrum was divided by the maximum value reached in the same spectrum. This procedure

therefore normalizes the maximum value in any spectra to a value of 1 in order to reduce variance resulting from differences in absolute peak intensity between replicate samples.

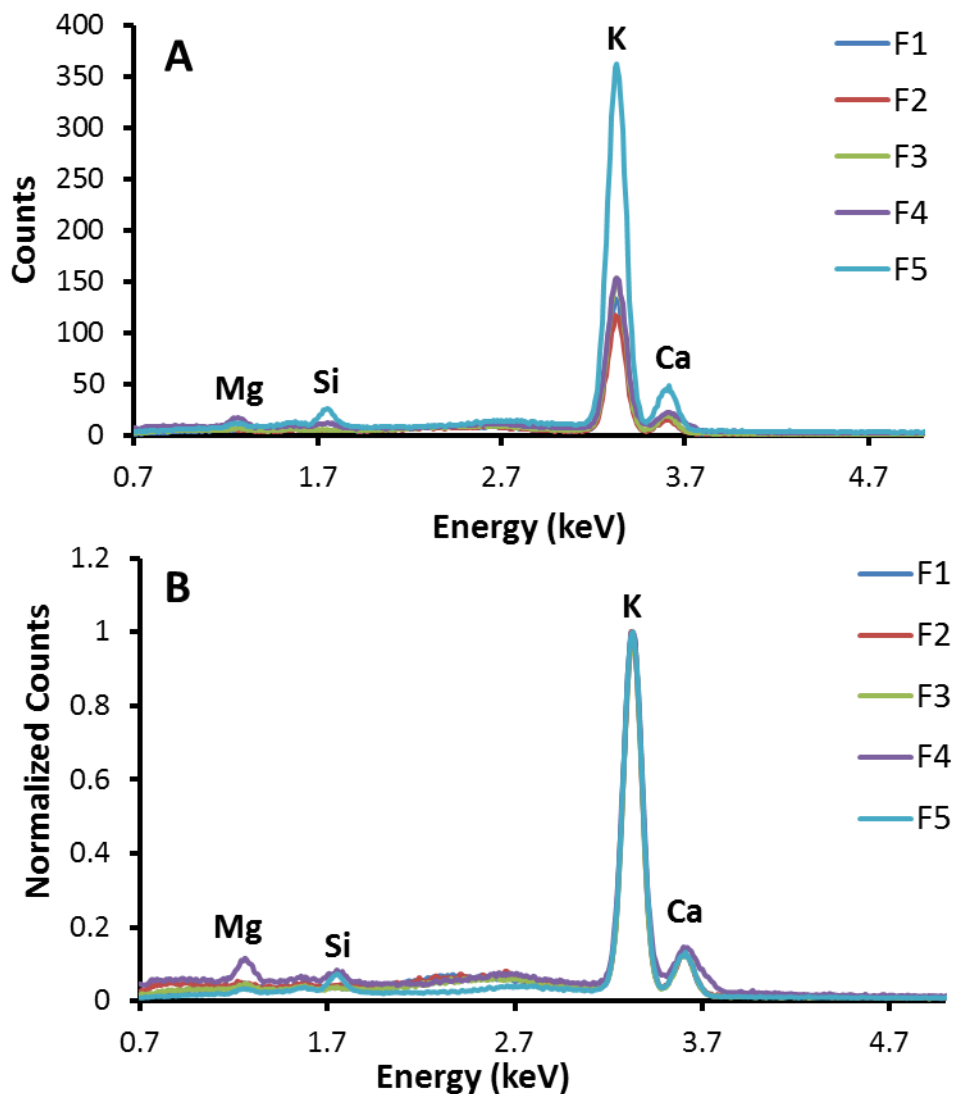


Figure 3.9: EDS spectra for the five replicate (F1-F5) firings of WinSC primers before (A) and after (B) maximum peak normalization.

Initially, PCA was performed on a data set consisting of the road flare and the five spectra of each of the six primers using commercially available software (The Unscrambler X,

version 10.1, CAMO, Woodbridge, NJ). Scores plots were generated with PC1 plotted on the x-axis and PC2 plotted on the y-axis and were used to assess the suitability of PCA for visualizing differences and similarities among the different primers and the road flare. Additionally, the loadings plots resulting from this analysis were also analyzed to help understand the variables (i.e., elements) contributing to the similarities and differences observed among the samples.

After assessing the applicability of PCA with the primer samples, the procedure was repeated using just the intact ammunition samples with the flare, and finally again with the entire data set (i.e., all five of the average firings of both the primers and intact ammunition along with the road flare). Scores and loadings plots were again used to explore the ability to visualize both underlying differences and similarities among different ammunition types, as well as between primer and intact ammunition of the same type. The positioning among replicates was compared both within primer and intact ammunition groups but also between primer and ammunition groups themselves.

REFERENCES

REFERENCES

- (1) Oommen, Z.; Pierce, S. M. *Journal of Forensic Sciences* **2006**, *51*, 509.
- (2) Steffen, S.; Otto, M.; Niewoehner, L.; Barth, M.; Brožek-Mucha, Z.; Biegstraaten, J.; Horváth, R. *Spectrochimica Acta Part B: Atomic Spectroscopy* **2007**, *62*, 1028.

CHAPTER 4: RESULTS AND DISCUSSION

4.1 Introduction

This thesis focuses on determining whether differentiation of lead-free ammunition is possible based on differences in elemental compositions among manufacturers. After obtaining six available lead-free ammunitions, five from each manufacturer were disassembled to remove the bullet and propellant leaving only the cartridge case containing the primer intact. Currently, scanning electron microscopy with energy dispersive X-ray spectroscopy (SEM-EDS) analysis of gunshot residue (GSR) evidence qualitatively examines the size, morphology, and elemental composition of suspected GSR inorganic particles. Since SEM-EDS only studies inorganic particles, the most significant contributors to GSR are the primer and the bullet.¹ Removing the bullet and firing only the primers uncouples the elemental contributions to inorganic GSR. Primers were discharged as discussed in chapter 3 depositing GSR particles on conductive carbon tabs. Similar particles were also captured using live-firing of intact ammunition and through the burning of a commonly available road flare. All samples containing suspected GSR were then analyzed by SEM-EDS to determine the elemental composition of the particles recovered after firing. The road flare was included to serve as an environmental source of particles which may be chemically and physically similar to strontium-based lead-free GSR. Principal components analysis (PCA) was then performed on each data subset (primer only, intact ammunition), as well as the entire dataset to explore the feasibility of differentiating

lead-free ammunition by manufacturer and against an environmental source with statistical confidence.

4.2 Particle Deposition Observations

Notable differences were observed in terms of deposited GSR particle density between samples from different manufacturers. For both intact ammunition and primer samples, clear trends were evident (Table 4.1). In both sets of samples, the Magtech Cleanrange (Mag) and CCI Blazer (CCI) produced a large number of detectable particles. Remington UMC Leadless (Rem) produced nearly twice as many particles when studied as a primer sample alone compared to the intact ammunition. Meanwhile, both Winchester Winclean (WinCI) and Winchester SuperClean NT (WinSC) along with Sellier & Belot Non-toxic (S&B) consistently resulted in low particle density samples as evidenced by the low particle counts. Comparing particle recovery across all five firings for each of the six ammunitions shows consistency as the relative standard deviation (RSD) in each case is < 30%.

However, it must be noted that the counts presented in Table 4.1 do not include particles found to consist primarily of copper as these particles were excluded from this study. Copper particles accounted for > 40% of particles discovered for both of the Winchester samples. Surprisingly, copper particles were generally < 20% of recovered particles for the higher density samples such as Mag and CCI. On one hand, the disparity in the percentage of particles comprised primarily of copper (based on maximum characteristic X-ray emission) between manufacturers suggests the exclusion of copper as a characteristic element may reduce the ability to discriminate samples. Yet, the presence of copper particles in samples

from all manufacturers indicates that copper may be too common an ingredient in many ammunition components to be useful for association and discrimination of samples.

Table 4.1: GSR particle counts for each of five replicates for six different intact ammunition and primer samples. Error on the average is reported as \pm one standard deviation.

Intact Ammunition	F1 [†]	F2	F3	F4	F5	Average	RSD [‡]
Rem	44	45	42	52	48	46 \pm 4	8%
WinCl	28	12	27	28	26	24 \pm 7	28%
WinSC	34	23	32	26	20	27 \pm 6	22%
Mag	60	63	44	63	36	53 \pm 12	23%
CCI	87	54	77	61	66	69 \pm 13	19%
S&B	27	34	22	28	24	27 \pm 5	17%
Primer Only	F1	F2	F3	F4	F5	Average	RSD
Rem	70	63	86	100	90	82 \pm 15	18%
WinCl	38	36	70	47	46	47 \pm 14	29%
WinSC	43	40	42	47	44	43 \pm 3	6%
Mag	58	87	67	87	72	74 \pm 13	17%
CCI	98	73	63	67	51	70 \pm 17	25%
S&B	53	37	35	35	35	39 \pm 8	20%

†: Firing #

‡: Relative Standard Deviation

On average, the intact ammunition studies found only 70% of the number of particles recovered during primer experiments. The only exception was for the CCI samples where a similar number of particles were recovered in both studies. In the other cases, the higher particle collection efficiency in the primer studies likely results from the lower force ejecting the GSR from the barrel. While primers are explosive, they are designed to ignite the propellant in order to provide the thrust required to fire a bullet, not to create much force on their own.

Thus, the average particle recovery should be lower in the intact ammunition study since the higher discharged particle velocity allows the particles to travel much further distances than the target designed to catch the particles. The extra velocity may also lead to particle penetration deep into adhesive films within the carbon tabs used for particle collection.

4.3 Energy Dispersive X-ray Spectroscopy Analysis and Comparison of Spectra

4.3.1 Remington UMC Leadless

EDS analysis of the Rem samples show an average particle primarily consists of aluminum (Al) with some potassium (K) and a small amount of silicon (Si) (Figure 4.1). Despite being the major peak present, Al is not listed as a component of Rem ammunition according to its material safety data sheet (MSDS). However, Oomen and Pierce previously analyzed Rem ammunition and found primer particles consisted of Al, Si, K, sodium (Na), calcium (Ca), and magnesium (Mg), which is in agreement with our conclusions despite the MSDS difference.² In comparing the EDS spectra before maximum peak normalization from primer only versus intact ammunition studies, the average count was lower for the intact studies but general spectral trends and peak ratios are conserved indicating that the bullet doesn't contribute meaningfully to the GSR analysis. Looking at each set of five firings shows considerable variability in the average X-ray counts. For this reason, maximum peak normalization was used to remove this variance before PCA.

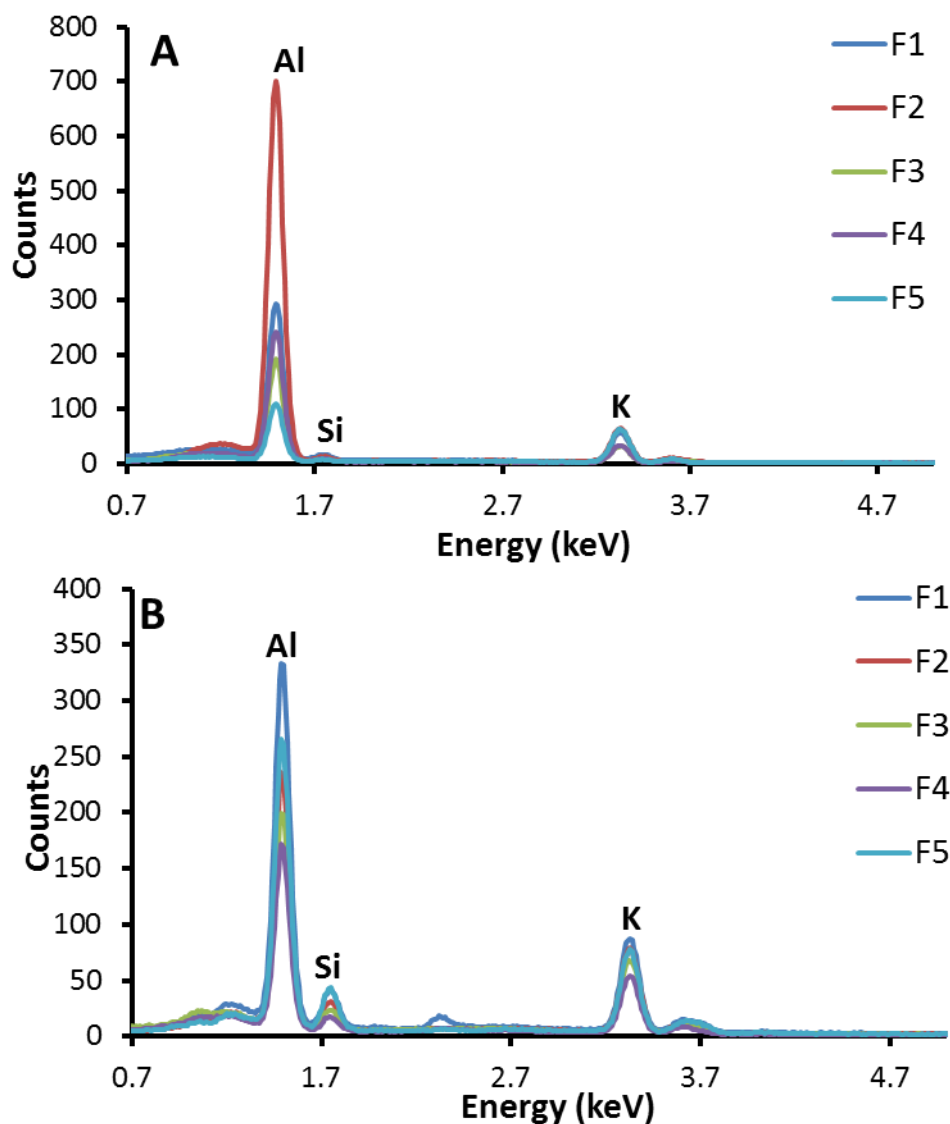


Figure 4.1: EDS spectra for the five replicate (F1-F5) firings of Rem primers (A) and intact ammunition (B) showing an elemental composition of Al, Si, and K, with Al as the dominant peak.

4.3.2 Winchester WinClean

EDS spectra of the WinCl samples indicate that the primer primarily consists of K as this was the only peak detected (Figure 4.2). For the intact ammunition, in one replicate trial Si actually was in higher abundance on average than K and small peaks corresponding to Na, Mg,

Al, S, and Ca were also observed. The large disparity in appearance of the spectra from primer and from intact ammunition suggests some influence on particle composition arising from the bullet or propellant. However, once again the work of Oomen and Pierce supports the observed results.² In their experiments, direct ignition of primers produced K dominated spectra with traces of Al, Si, calcium (Ca), and sulfur (S) among other elements. Similar to the Rem samples, K is not listed as a component on the MSDS for WinCl.

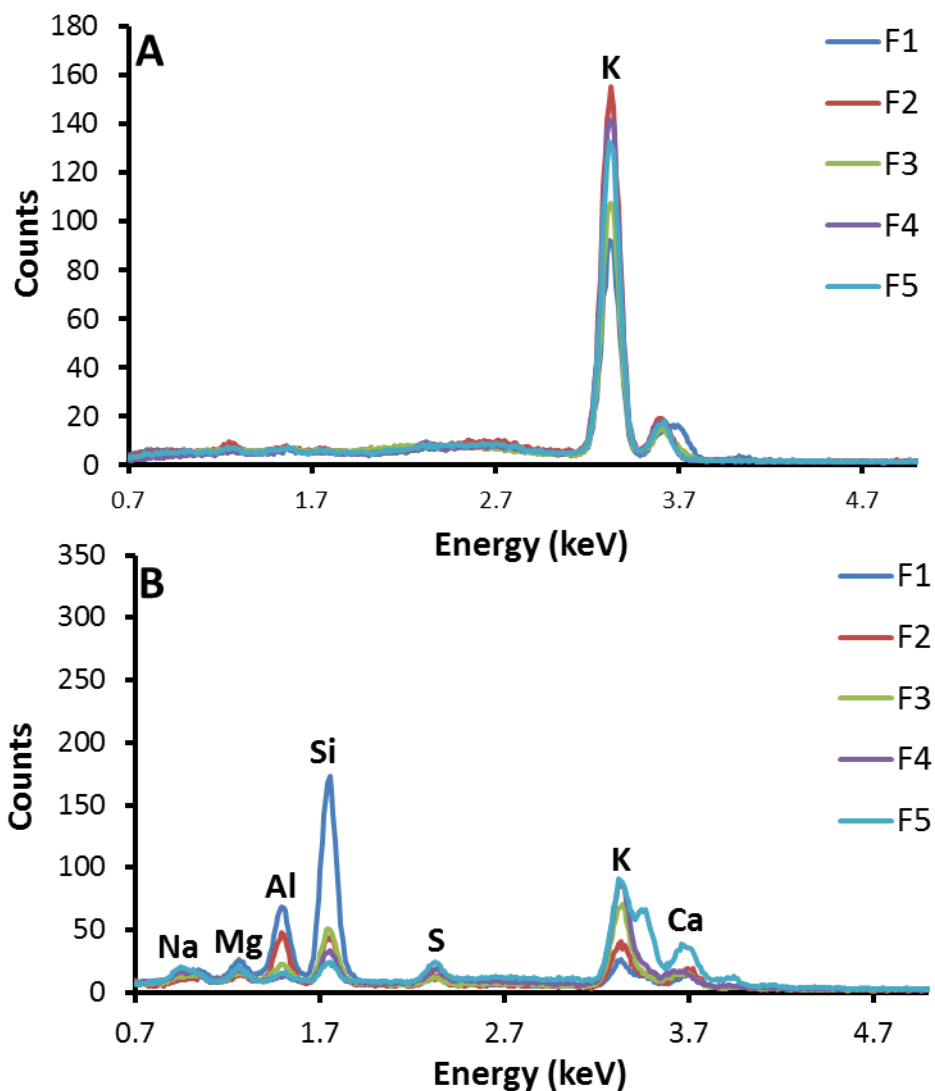


Figure 4.2: EDS spectra for the five replicate (F1-F5) firings of WinCI primers (A) and intact ammunition (B) showing an elemental composition of K and Si, K with traces of Na, Mg, Al, S, and Ca.

4.3.3 Winchester SuperClean NT

When comparing the EDS spectra observed for the WinSC samples to the WinCI samples, many similarities are evident. Once again, the primer only sample consists almost entirely of K with a slight trace of Si and the intact ammunition consists primarily of K with traces of Mg, Al, Si, S, and Ca like WinCI (Figure 4.3). However, the WinSC ammunition has not

yet been studied in any other publications. Of course, it is not particularly surprising that the composition of GSR produced by two different ammunitions made by the same company would be similar as many parts and components are likely used in both products. The MSDS provided by the manufacturer only lists tin, zinc, and Cu as inorganic components which cannot sufficiently explain all the elements observed by EDS.

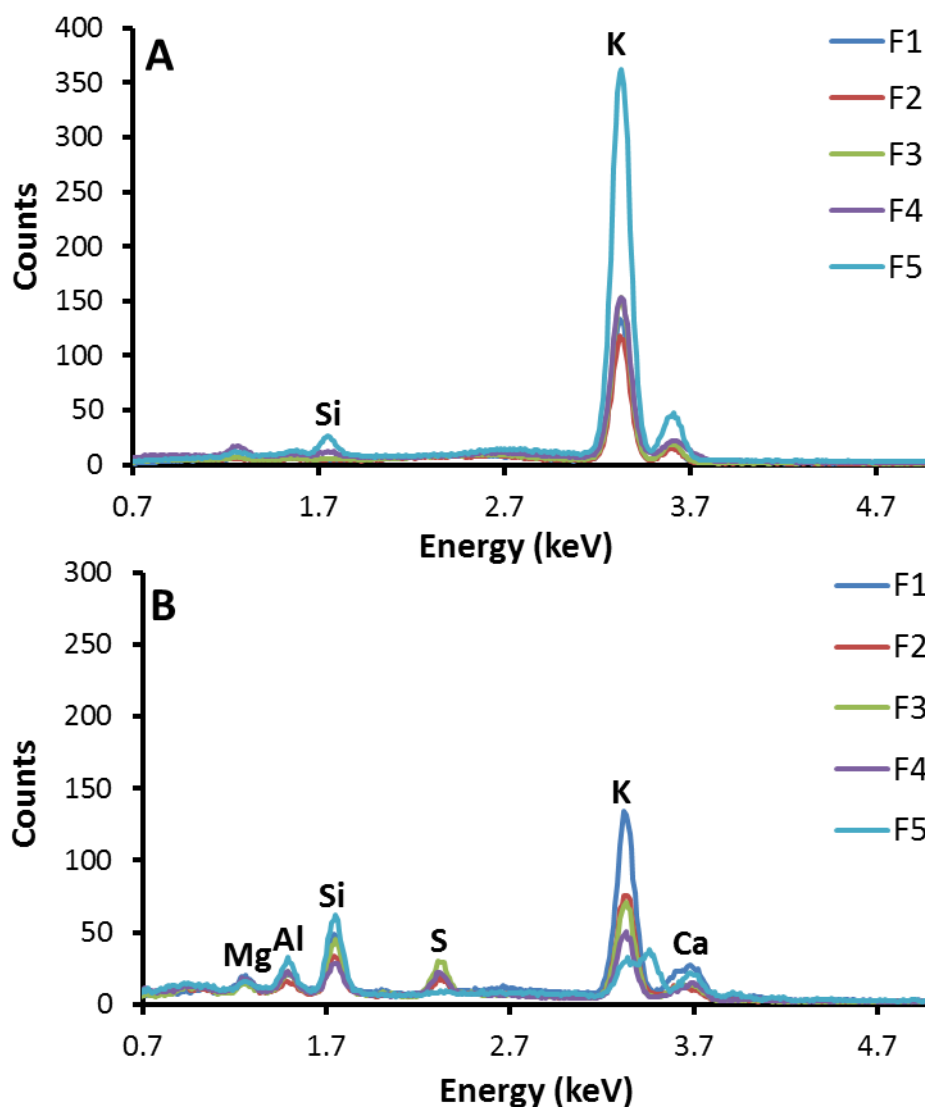


Figure 4.3: EDS spectra for the five replicate (F1-F5) firings of WinSC primers (A) and intact ammunition (B) showing an elemental composition of K and Si with traces of Mg, Al, S, and Ca.

4.3.4 Magtech Cleanrange

Mag appears to contain primarily Al and Si with a minor amount of K and a trace of Ca based on the EDS spectra for primer samples (Figure 4.4). Interestingly, there are relatively few differences between the primer and intact ammunition studies. However, in the primer samples, Si is the dominant peak while in the ammunition studies Al is dominant. This suggests that many of the GSR particles on the surface likely contain both Al and Si. However, in 2007, Steffen et al. demonstrated that on average, Mag ammunition was comprised of strontium (Sr) and hence, was similar in elemental composition to road flares.³ Yet, the results obtained in this study clearly do not support the same conclusion as not even trace levels of Sr were detected in Mag samples. Therefore, the manufacturer may have made changes to the formulation during the past 5 years leading to the difference in elemental composition observed.

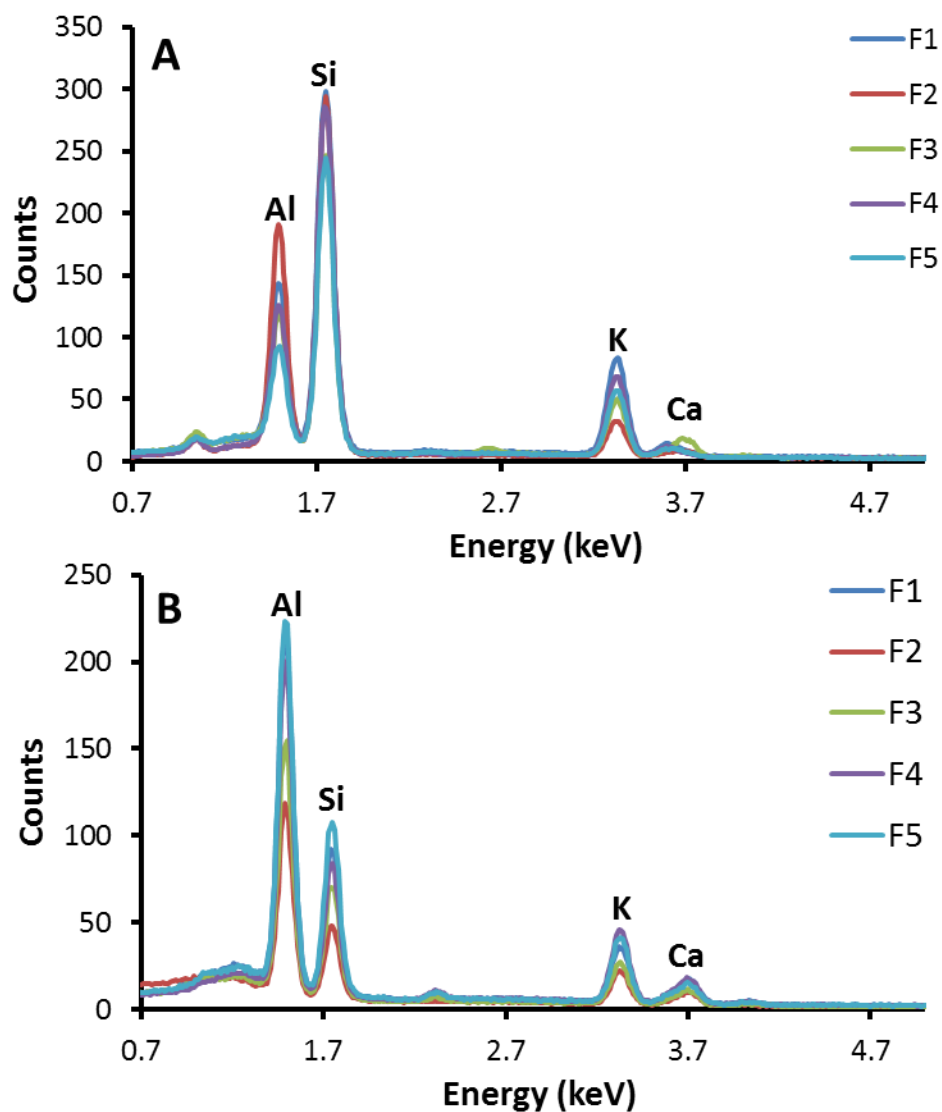


Figure 4.4: EDS spectra for the five replicate (F1-F5) firings of Mag primers (A) and intact ammunition (B) showing an elemental composition of Al and Si with traces of K and Ca.

4.3.5 CCI Blazer

Unlike the other ammunitions tested, CCI contains primarily Sr, with some contribution by Al based on the EDS spectra from the primers and the intact ammunition (Figure 4.5). This finding is in agreement with work by Steffen et al. which indicated that CCI is primarily

composed of Sr.³ The major difference between the primer samples and the ammunition samples is the ratio between Sr and Al as the amount of Al increased for intact ammunition. The cartridge cases for CCI are actually made from Al so the increased pressure and temperature present upon firing the intact ammunition should vaporize more Al leading to a higher concentration of Al in GSR particles.

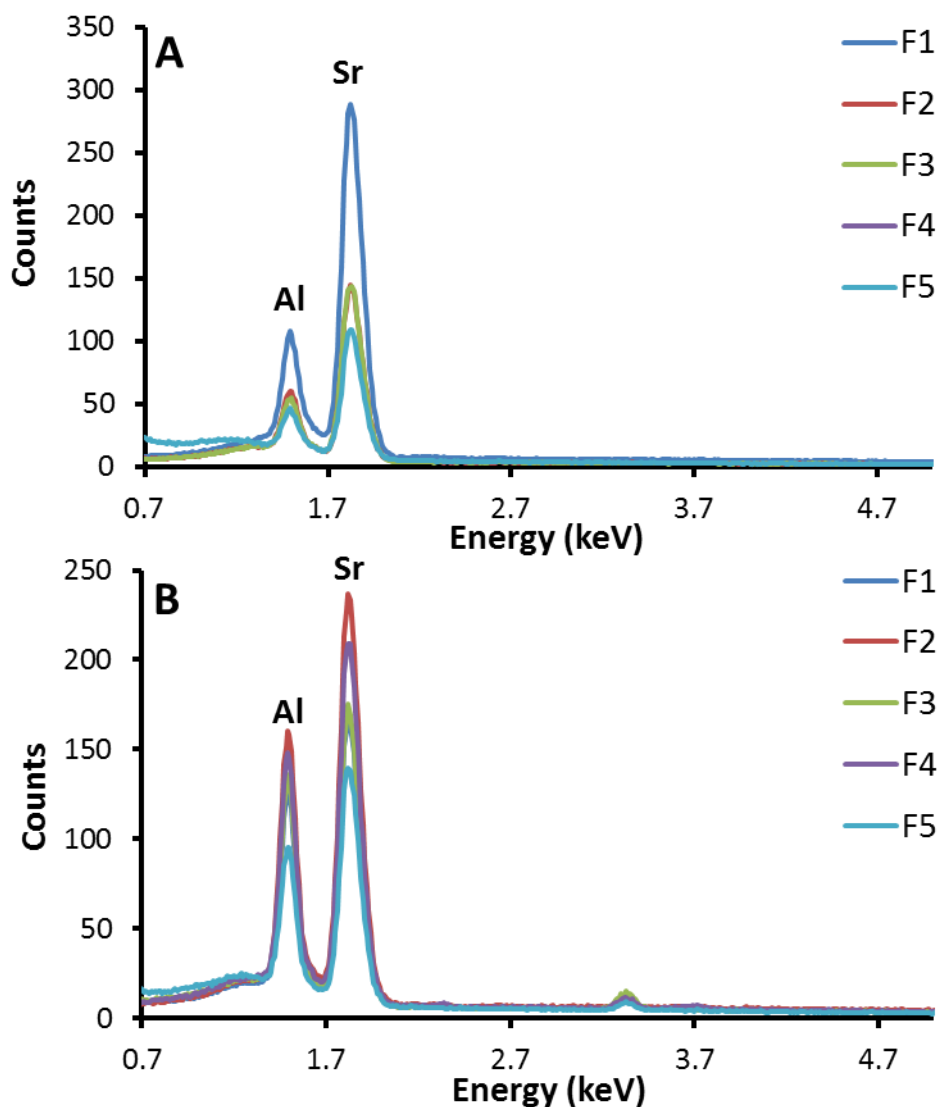


Figure 4.5: EDS spectra for the five replicate (F1-F5) firings of CCI primers (A) and intact ammunition (B) showing an elemental composition of Sr and Al.

4.3.6 Sellier & Bellot Non-toxic

Primer samples from S&B ammunition contain primarily Si with a trace of K present (Figure 4.6). Ammunition samples have a similar composition except with additional trace amounts of Al and Ca present in addition to the K. The high concentration of Si in GSR from S&B is logical due to the presence of glass within the primer along with a potassium salt. As before, the elemental composition of S&B in this study is generally in agreement with the results of Steffen et al., with the exception of the trace amount of Al found in this study but reported by Steffen et al.³

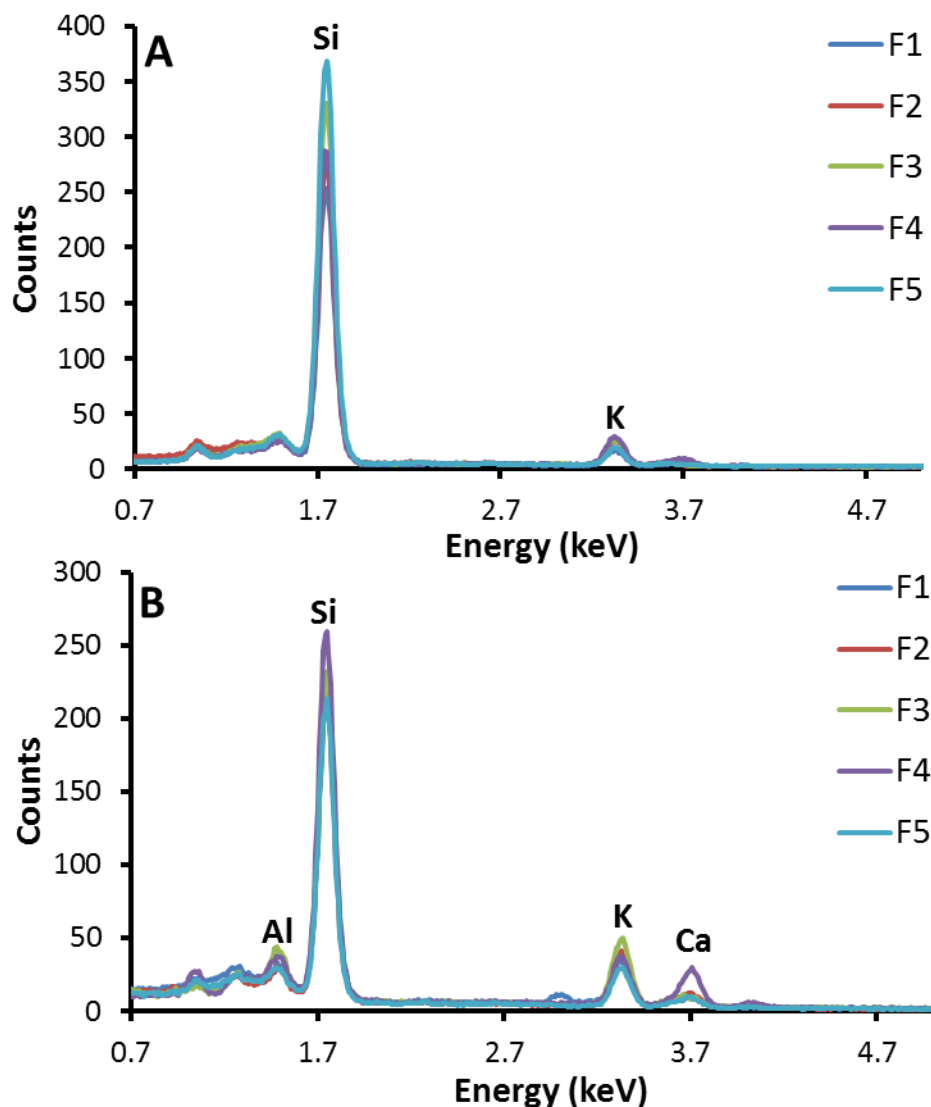


Figure 4.6: EDS spectra for the five replicate (F1-F5) firings of S&B primers (A) and intact ammunition (B) showing an elemental composition of Si with traces of Al, K, and Ca.

4.3.7 Orion Road Flare

EDS analysis of ORI revealed a composition similar to CCI with Sr as the primary element with traces of S, chlorine (Cl), and K (Figure 4.7). Each of these elements is logical to find in the discharged particles based on the MSDS contents claiming Sr, K, and Cl in the form of

perchlorate and chlorate, and S. Therefore, all of the inorganic elements which the manufacturer lists as being present within the flares were detected.

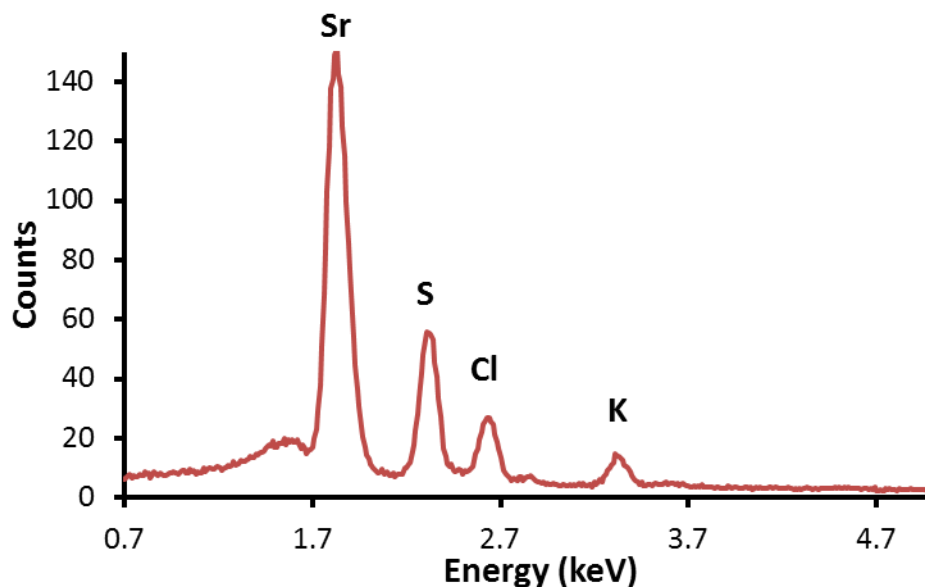


Figure 4.7: EDS spectrum for the particles resulting from burning an ORI flare showing an elemental composition of Sr and S with traces of Cl and K.

4.3.8 Comparison of Ammunition and Road Flare Based on EDS Spectra

Within each set of firings for a given ammunition type, especially for primer firings, the X-ray counts of the peaks shift slightly due to differences in the intensity or concentration of the elements detected. Since this study looks at average X-ray count values for an entire set of particles resulting from a single firing, the variability between firings is reasonable. X-ray count intensity is related to the size of the particle as the smaller a particle is, the more background is sampled by the EDS and incorporated into the resulting spectrum. Conversely, larger particles occupy a greater portion of the EDS analysis area resulting in higher X-ray counts for the elements present in GSR. However, the peak positions are fixed since the elemental

composition does not change. Therefore, comparing a single primer firing from each ammunition against the flare is reasonable to see if the samples can be visually discriminated based on elemental composition alone (Figure 4.8). For such a visual comparison, the magnitude of the X-ray count is not considered important but rather the X-ray energies are important since they provide information about which elements are present. Based on a visual comparison of the overlaid spectra, WinCl, WinSc, and Rem can be excluded as being similar to the road flare. All three lack any peaks in the vicinity of Sr and are therefore easily distinguished by eye. Additionally, WinCl and WinSc contain a small Ca peak and Rem primarily consists of Al, neither of which is present in samples from ORI.

Spectra for S&B and Mag both have strong peaks corresponding to Si which overlap with the peak arising from Sr. These two ammunition types also have a similar ratio between the K intensity and the Si peak intensity, leaving their visual discrimination reliant on a woefully subjective analysis based on the intensity of the Al peak present. The high elemental similarity between Mag and S&B presents a significant challenge for visual discrimination. However, as spectra for both ammunition types lack a peak corresponding to Sr, a trained analyst should be able to distinguish Mag and S&B from a road flare sample.

The most challenging sample to distinguish from the road flare is the CCI ammunition as both CCI and ORI have Sr as the primary peak. Yet, the strong response from S, Cl, and K can distinguish ORI as being visually different than CCI despite sharing the primary Sr peak. Hence, visual discrimination of EDS results by trained analysts is still a suitable method for differentiating lead-free ammunition GSR. However, the ability to use PCA to draw out

underlying differences and similarities among the samples could provide a statistical confidence on whether particles arose from the same source. The ability to use statistical comparisons, such as t-tests, with PCA results removes a substantial portion of the subjectivity involved in analyst-based visual spectral matching. However, as this work serves only as a preliminary investigation into the use of PCA for lead-free GSR analysis, t-tests were not employed for association and discrimination between manufacturers since visual discrimination of PCA results was typically sufficient. Additionally, discrimination of ORI by t-tests was not possible since only one flare was analyzed and a mean value was not established.

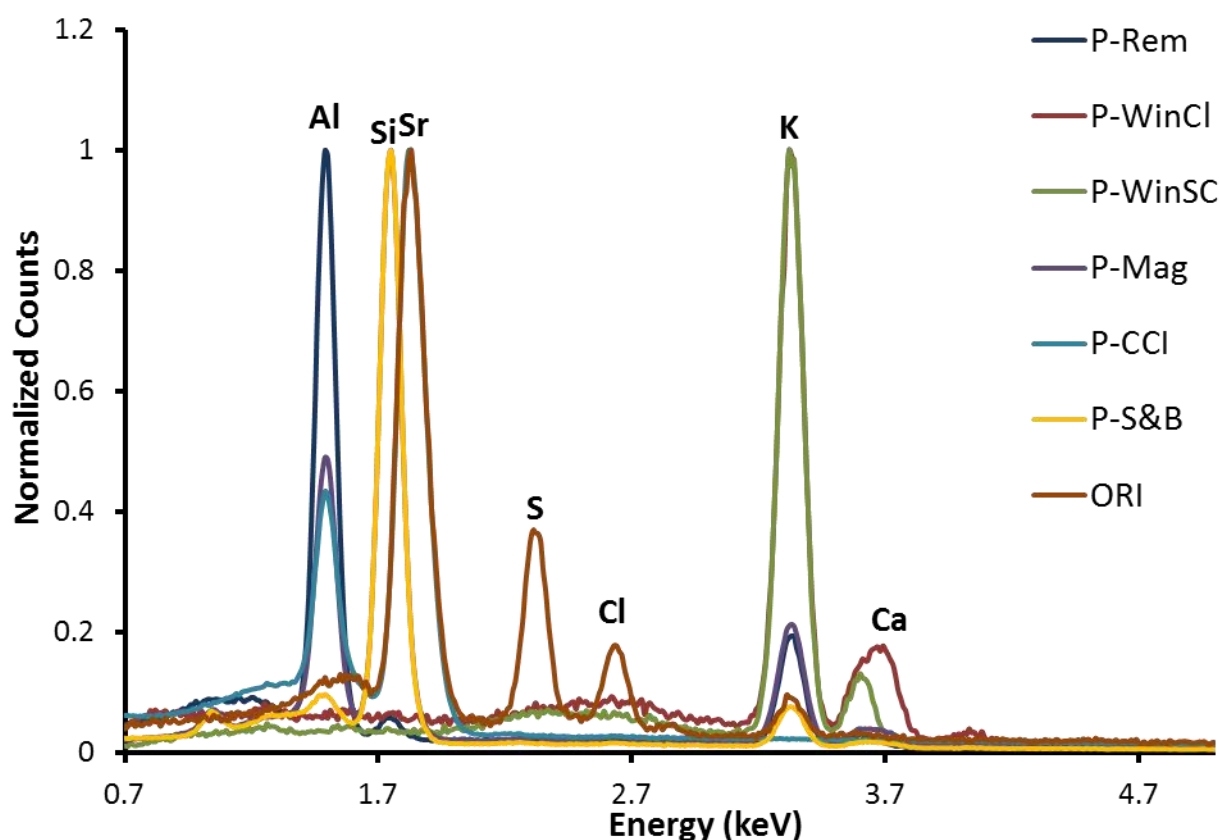


Figure 4.8: Overlaid average EDS spectra comparison of a single replicate trial from each ammunition compared to the ORI spectrum to assess whether road flares may be visually discriminated from lead-free ammunition on the basis of EDS elemental composition.

4.4 Principal Components Analysis

4.4.1 Primer Samples and Road Flare

Despite some visual differentiability among the primer samples and the road flare, the replicate EDS spectra from all six ammunitions and the road flare were further analyzed by PCA. PCA can exploit the discriminatory value of small emission differences within the energy spectrum monitored (0.7-5 keV) and allow statistical confidence intervals to remove the subjectivity arising from visual association and discrimination of samples. PCA allows observation of the similarities and dissimilarities present in the data set and should correspond well with the visual differentiation attempted earlier in this chapter. The PCA results were visualized using a scores plot comprised of the first two principal components (PCs) which accounted for 78% of the variance within the dataset (Figure 4.9). A scores plot is used to show the relationship between samples and the PCs determined correspond to the greatest sources of variance with the dataset. Samples may position positively or negatively along each PC based on whether they contain variables which contribute positively or negatively to the variance in each PC. Samples which are chemically similar generally position near one another. For this reason, the five firings for each primer are observed to overlay upon each other. This tight positioning prevents discrimination of P-WinCl and P-WinSC and challenges discrimination between P-S&B and P-Mag. The spread in the positing of P-Rem and P-Mag results from chemical dissimilarities between the firings. The positioning of the samples was evaluated based on the information about which variables (in this case elements) are contributing most to the variance using the loadings plots (Figure 4.10).

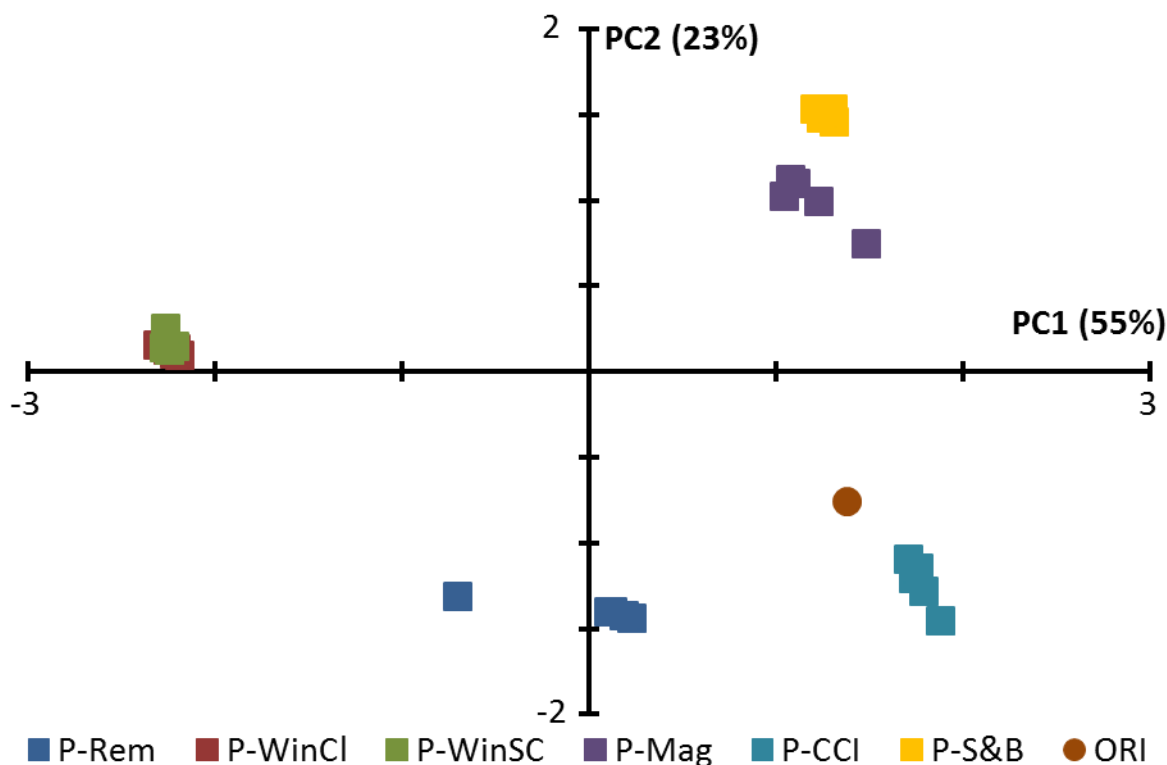


Figure 4.9: PCA scores plot showing clustering of replicate primer samples for the six ammunitions and the positioning of the road flare sample.

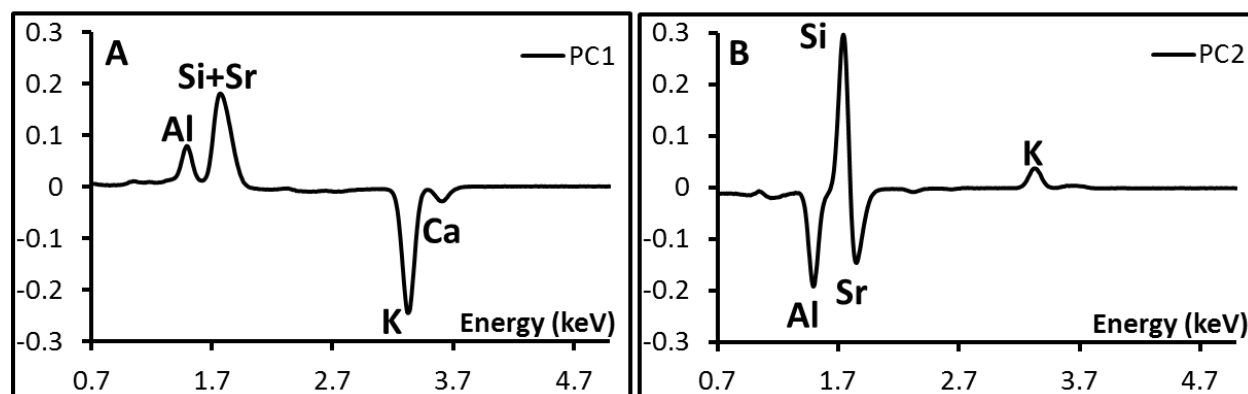


Figure 4.10: PCA loadings plots showing each element's contribution to the variance corresponding to PC1 (A) and PC2 (B).

Loadings plots are used to indicate which portions of the spectra (elements) are contributing to the variance in the dataset. PC1 accounts for the largest portion of the variance

within the dataset and the loadings on PC1 show that Al, Si, and Sr all weight positively while K and Ca are weighted negatively on PC1. Proceeding to PC2, accounting for the second highest amount of variance in the data set, Si and K now weight positively while Al and Sr weight negatively. Once the contribution each element makes to the variance is identified through loadings plots, the positioning of samples on the scores plot can be explained based on the elemental composition.

First, the PC1 loadings plot indicates that Si or Sr weight positively so samples containing these elements, such as P-Mag, P-CCI, P-S&B, and ORI, position positively on PC1 in the scores plot, while samples with K as the primary peak position negatively (P-WinCl, P-WinSC). Similarly, since Al only contributes slightly to the positive loading in PC1, P-Rem samples position near zero as they contain only Al and a trace of K. The negative weighting of K on PC1 may counteract any slight positive weighting provided by Al. Likewise, loadings in PC2 show positive weighting for Si and K indicating samples that contain Si or K position positively while samples with Al and Sr position negatively in the scores plot. The largest spread in replicates along either PC occurs for the P-Rem series along PC1 and can be explained by looking at the normalized EDS spectra (Figure 4.11). The elevated X-ray counts from K in the fifth firing leads to more negative weighting on PC1 causing this point to be positioned more negatively on PC1 than the other replicates in the scores plot.

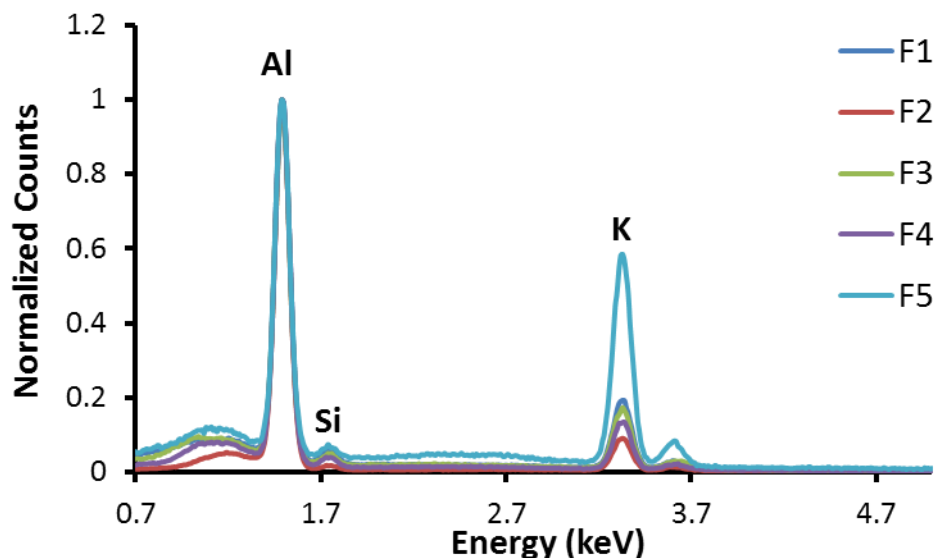


Figure 4.11: Normalized average EDS spectra for P-Rem showing the fifth firing with increased K content compared to the other four firings.

Examining the position of ORI shows an overlap in PC1 on the scores plot with P-Mag and P-S&B indicating no differentiation between the samples on this principal component. The overlap results from the combined Si and Sr peak present in the loadings plot for PC1 (Figure 4.10 A). Recall that both P-Mag and P-S&B contain intense peaks for Si while road flares produce similar peaks for Sr. Due to the energetic similarity in peaks from Si and Sr discussed earlier in this chapter, PCA combined the two peaks into a single variable as seen in the loadings plots for PC1. However, from the PC2 loadings plot, Si is weighted positively while Sr is weighted negatively and therefore, distinction of these samples is possible as P-Mag and P-S&B are positioned positively, while ORI is positioned negatively, on the scores plot. The closest primer grouping to ORI comes unsurprisingly from P-CCI since both contain Sr as the primary peak. However, the Al present in P-CCI leads to a slight increase in positive positioning on PC1 and negative positioning on PC2 relative to ORI. The small K peak present in ORI also leads to a

slightly more negative positioning on PC1 and more positive positioning on PC2 compared to P-CCI. With the assistance of the two smaller peaks present in the spectra, ORI and P-CCI position separately on the scores plot, albeit only slightly.

4.4.2 Intact Ammunition Samples and Road Flare

PCA was also used to examine differences between the intact ammunition samples and the road flare in a similar manner to that which was done with the primer samples. Intact ammunition is more likely to be encountered in forensic evidence and is also more complicated due to extra contributions to the GSR arising from the propellant or bullet. Once again, a scores plot was used to visualize results in the first two principal components, which described 69% of the variance in the data set (Figure 4.12). The positioning of the samples in the scores plot was also examined by determining the variables contributing most to the variance using the loadings plots (Figure 4.13).

Like before, firings from the same ammunition positioned near one another on the scores plot. However, WinCI and WinSC show increased spread in both PC1 and PC2. This increased spread likely results from differences in the counts of the many trace peaks corresponding to Na, Mg, Al, S, and Ca present in these two samples. The positioning of firings in new locations arises from the fact that different variables contribute strongly to the variance in this dataset compared to the primer only samples.

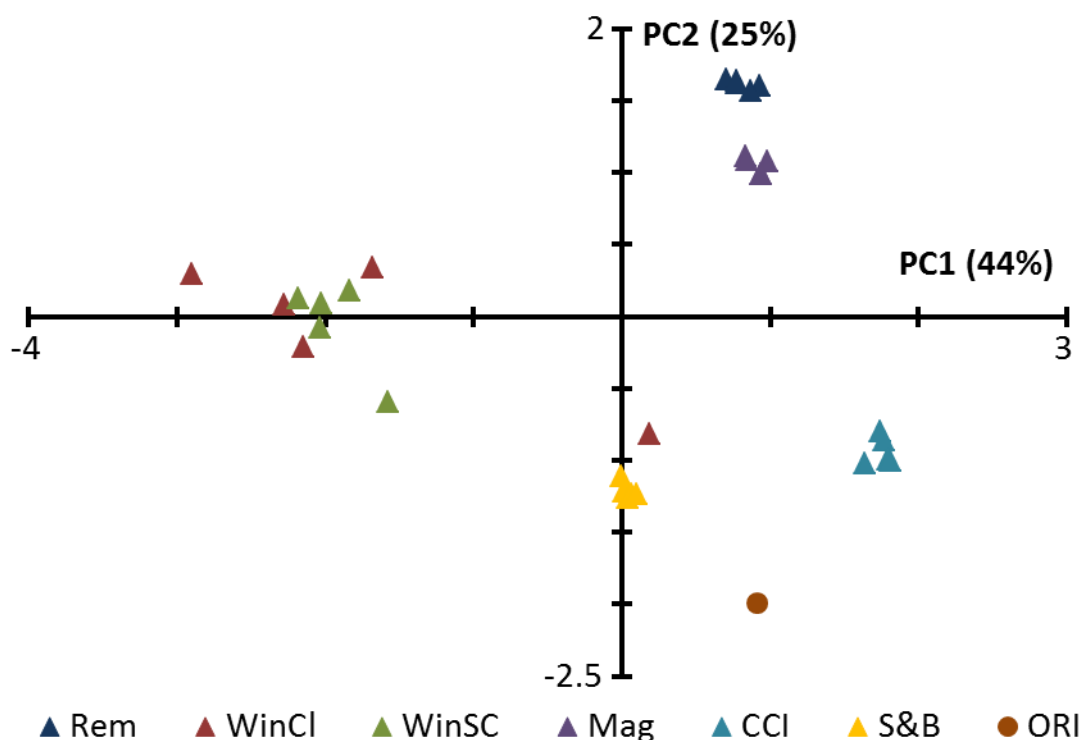


Figure 4.12: PCA scores plot showing clustering of intact replicate samples for the six ammunitions and the positioning of the road flare sample.

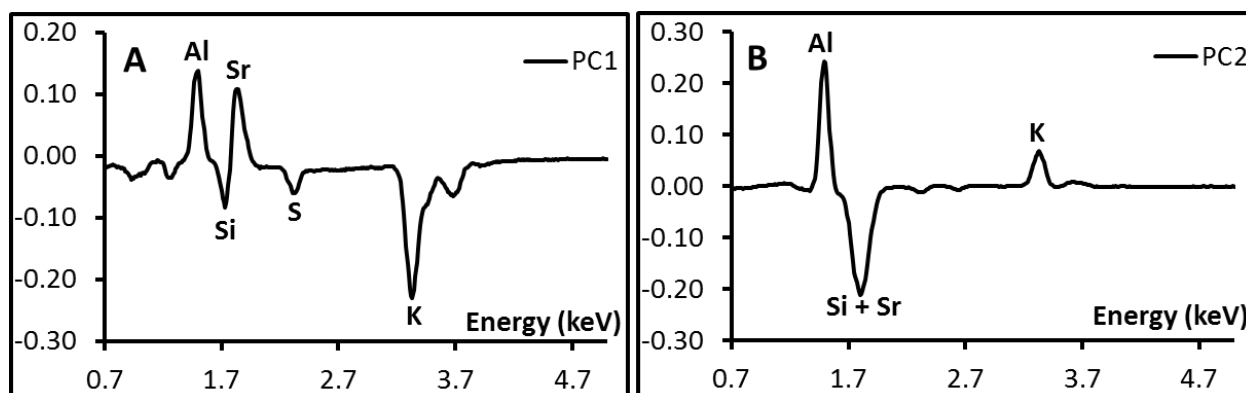


Figure 4.13: PCA loadings plots showing contributions to the variance corresponding to PC1 (A) and PC2 (B).

The loadings plot for PC1 shows Al and Sr are weighted positively while Si, S, and K are all weighted negatively. Meanwhile, for PC2 the loadings show that Al and K are weighted

positively and a combination peak from Si and Sr is weighted negatively. The high content of Sr and Al in CCI ammunition leads to the positive positioning on PC1 while the excess Sr content leads to negative positioning in PC2. For the case of S&B, Si does not contribute much to the variance in PC1 based on the loadings plot but does contribute in PC2 leading to negative positioning of S&B on PC2 without an effect in PC1. The Sr and K present in ORI lead to a positive positioning on PC1 and the excess Sr content also leads to negative positioning on PC2. However, ORI is positioned far enough away from CCI and S&B for reasonable discrimination.

4.4.3 Complete Dataset and Road Flare

Finally, PCA was used to analyze the dataset comprised of all firings for primer only and intact studies, as well as the ORI sample in order to assess association and discrimination between primer samples and intact ammunition along with the road flare. Just as before, the scores plot was examined using PC1 and PC2, which for this data set accounted for 67% of the variance (Figure 4.14). Likewise, the positioning of replicate firings on the scores plot was analyzed through use of the loadings plots to determine which variables were contributing the most to the dataset variance (Figure 4.15).

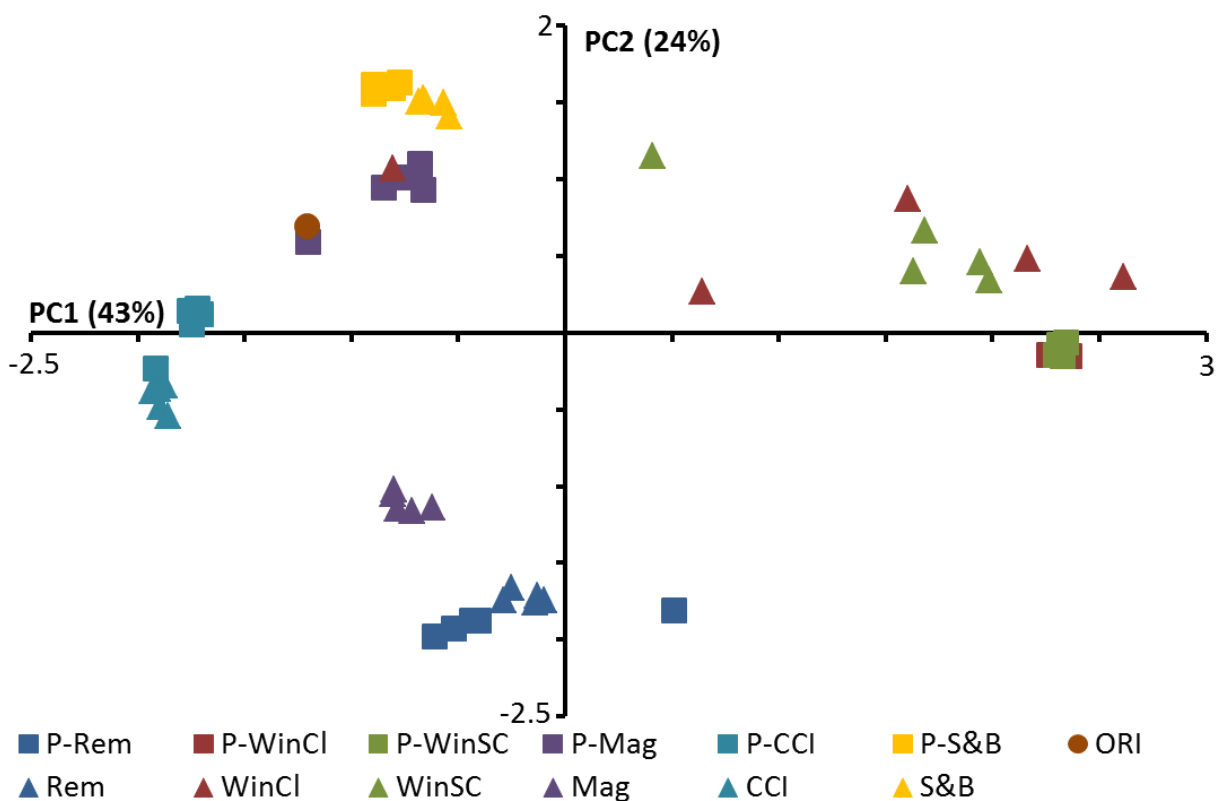


Figure 4.14: PCA scores plot showing clustering of intact and primer replicate samples for the six ammunitions along with the positioning of the road flare sample. Square symbols denote primer samples while triangles denote intact ammunition samples.

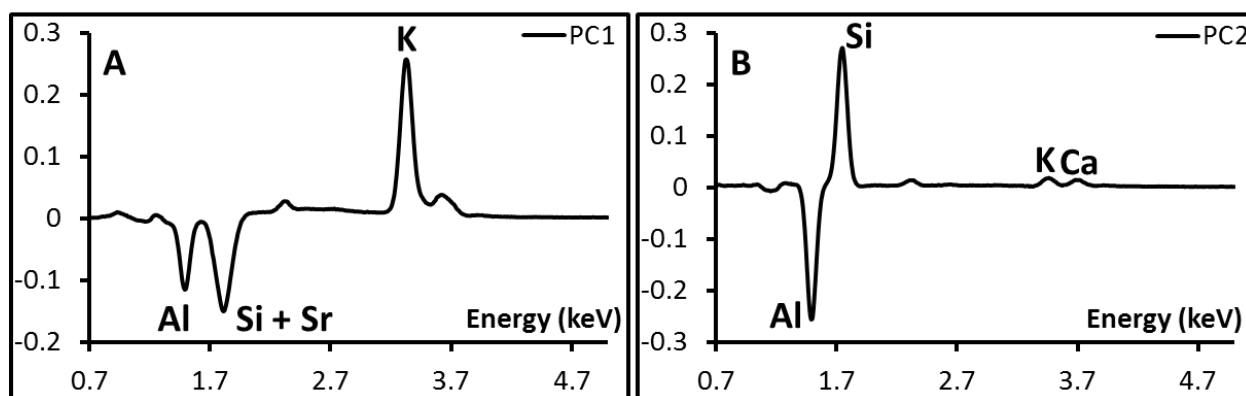


Figure 4.15: PCA loadings plots showing each element's contribution to the positioning on PC1 (A) and PC2 (B).

This time the scores plot shows less discriminatory ability than for the primer or intact ammunition firings alone based on increased spacing among firing groups and overlap in positioning between unrelated firings. The WinCl and WinSC ammunition samples in particular are not well positioned near the primer samples or even each other in this scores plot. In fact, a replicate of WinCl even overlaps in position with several firings of P-Mag. Similarly, the only firing of P-Mag to not cluster with the rest overlaps in position with ORI, hindering discrimination. The scores plots now show that Al, Si, and Sr all weight negatively on PC1 while K weights positively. Similarly, Si, K, and Ca all weight positively on PC2 while Al weights negatively.

Looking at the scores plot for the combined dataset, primer sample replicates position near one another as was seen earlier in the chapter. In the case of Rem, Mag, CCI, and S&B the intact ammunition replicates also closely positioned to their respective primers, presumably due to similarities in the spectra. However, spread between firings for WinCl and WinSC in the intact studies only increased when moving to the combined dataset due to the dissimilarity between the EDS spectra for the primer samples and those corresponding to the intact ammunition. As expected from the loadings plots, samples with intense K peaks (WinCl, WinSC) positioned positively on PC1 while other samples containing Al or Sr (CCI, Rem) positioned negatively. Similarly, PC2 differentiated samples based on their Al or Si content, with samples containing Al positioning negatively and samples containing Si positioning positively on PC2.

Once again, a positioning anomaly was observed, in this case for Mag. Both the primers and the intact replicates positioned similarly along PC1 but were spread in PC2 despite being

closely positioned among replicates. Looking at the original EDS spectra for P-Mag and Mag explains the difference in loading in PC2 succinctly (Figure 4.4). The primer samples produced average spectra with Si as the dominant peak while the dominant peak in the intact ammunitions was Al. Looking at the loadings on PC2, Al loads negatively and Si positively causing the separation between the two studies' replicates despite their reproducible average particle composition within each set. Additionally, ORI positioned similarly in both PC1 and PC2 to a firing from P-Mag, preventing visual discrimination of the flare from the ammunition. However, a closer inspection of the original EDS spectra for those two revealed a different major peak for each with Si being the major peak for P-Mag and Sr for ORI. In this way, the two average spectra could still be distinguished, albeit without any of the statistical benefits hopefully possible through PCA.

This chapter discussed the ability to visually associate and discriminate lead-free ammunition and determined that, due to large differences in composition between some manufacturers, visual differentiation based on EDS may be possible. However, Mag and S&B shared highly similar elemental profiles complicating visual differentiation between the two. The use of PCA allows extraction of underlying variance from the dataset which may better help differentiate EDS results with similar compositions and also allows for the use of statistics to assign confidence to associate and differentiate samples. PCA was suitable for analysis of primer firings but was more challenged when using the combined dataset consisting of both the primers and intact ammunition with the road flare due to increased spread in the firings. The spread likely resulted from the large elemental compositional differences observed between some primer and intact-ammunition characterization studies.

REFERENCES

REFERENCES

- (1) Wallace, J. S. *Chemical Analysis of Firearms, Ammunition, and Gunshot Residue*; CRC Press: Boca Raton, FL, 2008.
- (2) Oommen, Z.; Pierce, S. M. *Journal of Forensic Sciences* **2006**, 51, 509.
- (3) Steffen, S.; Otto, M.; Niewoehner, L.; Barth, M.; Brožek-Mucha, Z.; Biegstraaten, J.; Horváth, R. *Spectrochimica Acta Part B: Atomic Spectroscopy* **2007**, 62, 1028.

CHAPTER 5: CONCLUSIONS AND FUTURE WORK

5.1 Conclusions

Elemental classification of GSR particles coupled with multivariate statistical procedures may yet still advance traditional GSR analysis procedures, in line with growing demands from the judicial system. This thesis covered two different studies assessing the feasibility of the analysis of lead-free GSR samples from primers and intact ammunition using SEM-EDS and with PCA for statistical analysis of the data. In the first study, bullets and propellants were removed from ammunition to leave only primers and cartridge casings behind. These isolated primers were discharged, expelled GSR particles were collected, and the collected particles were directly analyzed by SEM-EDS. A representative number of particles from each of five replicate firings were characterized to assess the elemental distribution of the GSR samples. Due to a high variability in elemental composition, all particles collected during a firing were averaged to form an overall particle composition corresponding to each firing. This was necessary to reduce the large variance in individual particle composition that may otherwise prevent association and discrimination of samples using PCA. Experiments were then similarly repeated using intact ammunition to incorporate GSR contributions from the propellant and bullet to compare directly with results from the isolated primers.

When possible, elemental compositions of particles determined in this study were compared against previously published characterizations of identical brands or company issued MSDS to ensure consistent and trustworthy results. In all studied ammunitions except for

Magtech Clean Range, this study reproduced elemental compositions similar to those reported previously. In the case of the Magtech ammunition analyzed in this study, no Sr was present although this element had previously been reported as a component in the same ammunition. Such a discrepancy suggests that, in the time between the two studies, there is the possibility that the manufacturer switched from a Sr-based primer system to a Si, Al, and K formulation, similar to the formulation used in several other lead-free ammunitions.

PCA demonstrated the ability to associate firings of the same ammunition type, associate different ammunitions using a common primer, and to differentiate ammunitions using different primers. In the study involving primer GSR residues, differentiation of different ammunitions and a road flare, a common source of particles with similar chemical composition to those found in non-toxic ammunition, was possible based on visual assessment of the scores plot. When analyzing a combined dataset consisting of firings of the primer alone, as well as the intact ammunition, primer replicate firing positioning remained tightly grouped while ammunition samples visually were less associated. The spread in intact ammunition replicate firing groupings may result from the exclusion of Cu particles from this analysis since they were determined to be non-specifically located in most of the ammunitions studied. Several PCA positioning anomalies were discovered during testing, but all were easily explained by comparing the original EDS spectra with the loadings plots calculated during PCA.

While the ability to use statistical confidence intervals to describe the association and dissociation of GSR samples makes PCA an attractive technique, in the case of the lead-free ammunitions studied in this thesis, visual differentiation of all samples was possible due to

noticeable differences in elemental abundance. For this reason, it may be difficult to convince firearms and toolmark analysts to transition to using multivariate statistical techniques such as PCA without more illustrative examples of its benefits.

5.2 Future Work

The most immediate future opportunity for this study would be to go back through and not remove copper particles from analysis to see what effect this may have on the association and discrimination of samples, especially for intact ammunitions. Despite an initial hypothesis that copper would appear similarly between manufacturers since it is a common ingredient both in bullet jacketing and shell casings, the results showing higher copper particle recovery from certain ammunitions over others suggest this may not be so clear an assumption. If the Winchester rounds preferentially produce copper particles, then these particles could help to associate Winchester rounds between firings by increasing the number of particles incorporated into a more accurate average particle composition. Likewise, use of copper particles may also facilitate discrimination of Winchester rounds from other lead-free ammunition which may not produce as many copper GSR particles.

While lead-free (non-toxic) ammunition is considerably understudied in scientific literature compared to traditional ammunition, the high degree of variation in elemental formulation may be a doubled-edged sword. On one hand, the large number of formulations requires extra analysis time by forensic examiners to determine whether suspected GSR particles did in fact result from a shooting situation rather than unrelated, benign activities

(e.g., lighting a road flare). However, the disparity in formulations between manufacturers also allows for easier discrimination between available brands for purchase which may allow investigators to quickly focus in on a particular brand of ammunition likely used in a shooting occurrence.

All things considered though, the ability to differentiate GSR samples from lead-free ammunitions visually due to differences in elemental composition may reduce the usefulness of PCA for analysis. However, the firearms and toolmarks field as a whole must transition to more mathematically rigorous comparison procedures and the use of PCA or other multivariate statistical techniques for traditional lead ammunition may yet fill this need. The ability of PCA to draw out underlying differences from data sets could be helpful for magnifying small elemental abundance differences in ammunitions which all contain similar compositions. Additionally, the ability to extract more information from recovered GSR evidence, such as weapon caliber¹, based solely on small differences in elemental composition arising from contributions from barrel or other components of individual firearms may be possible through the combination of sensitive analysis techniques such as EDS or optical spectroscopy with PCA. The ability to use recovered GSR evidence during an investigation to provide leads even when a bullet may not have been recovered from a crime scene may expand the importance of ballistic evidence to law enforcement.

REFERENCES

REFERENCES

- (1) Bueno, J.; Sikirzhytski, V.; Lednev, I. K. *Analytical Chemistry* **2012**, *84*, 4334.